

C.6

CREEP OF TANTALUM UNDER CYCLIC
ELEVATED TEMPERATURES

by

Robert Lester Hammel

A Thesis Submitted to the
Graduate Faculty in Partial Fulfillment of
The Requirements for the Degree of
MASTER OF SCIENCE

Major Subject: Nuclear Engineering

Approved:

Signatures have been redacted for privacy

Iowa State University
of Science and Technology
Ames, Iowa
1960

TABLE OF CONTENTS

I.	INTRODUCTION	1
II.	REVIEW OF THE LITERATURE	3
	A. Creep Process	3
	1. Constant temperature conditions	5
	2. Cyclic temperature conditions	6
	B. Mechanical Properties of Tantalum	13
III.	OBJECTIVES OF THE INVESTIGATION	16
IV.	ANALYTICAL RELATIONSHIPS	17
V.	MATERIAL	22
VI.	EXPERIMENTAL PROCEDURES AND EQUIPMENT	29
	A. Testing Equipment	29
	B. Specimen Preparation	47
	C. Discussion of the Variables Introduced by the Techniques	49
VII.	RESULTS	57
	A. Creep Curves	57
	B. Evaluation of the Material Parameters	60
	C. Application of the ϕ Parameter	63
	D. Metallography	66
VIII.	DISCUSSION AND CONCLUSIONS	75
IX.	SUGGESTED TOPICS FOR FUTURE INVESTIGATION	78
X.	LITERATURE CITED	79
XI.	ACKNOWLEDGMENTS	82

I. INTRODUCTION

Creep is the plastic deformation of a material which occurs as a function of time and results from a stress being maintained over an extended period. The rate at which the deformation occurs for a given stress is highly influenced by the temperature condition. While the designer is usually concerned with creep at elevated temperatures, it also occurs and is often important at lower temperatures.

Technological advances have imposed very severe service conditions upon structural parts. This has resulted in considerable effort being expended in the search for materials possessing good mechanical properties at elevated temperatures. To develop such metals, it is recognized that a better understanding is needed of the mechanisms which lead to mechanical failure. The complexity of the problem is apparent when it is observed that even after years of investigation in the field, no general theory of creep exists, and investigators must satisfy themselves with certain experimentally observed laws.

Tantalum, because of its high melting point ($\sim 3000^{\circ}\text{C}$) and ability to withstand various corrosive environments, has received consideration as a material suitable for high temperature applications. It is being used in reactor loop studies (1) and in numerous process container applications. The determination of its mechanical properties has received

some attention in recent years but large gaps in the information exist.

It has been noted that a cyclic temperature condition can markedly alter the strain behavior of material as compared to that obtained under constant temperature conditions. In a nuclear reactor and indeed most applications where creep of a structural part is to be considered, a temperature variation of some form will occur during the service life.

The concept that creep is a thermally activated process, as developed by Dorn (2), provides the basis for the analytical equations used in this investigation to represent the creep of tantalum under constant and cyclic temperature conditions.

II. REVIEW OF THE LITERATURE

A. Creep Process

In general terms, Dorn states (2) that creep is a time-rate phenomena which is known to be highly temperature sensitive, dependent upon the previous history incurred by the material, and is attended by certain structural changes of the material as the strain progresses. A qualitative, much less a quantitative, treatment of these changes is difficult because of the complex nature in which they occur. Limited success along these lines has been achieved using single crystals.

For many materials Fig. 1 represents the characteristic creep curve observed experimentally. Initially the strain rate decreases from the time of loading until it achieves a constant value where the strain-time relationship is linear. Following this region the strain rate begins to increase and ultimately fracture of the specimen occurs. The first stage is an adjustment period in which the material is adapting itself in response to the load. The second stage is an equilibrium period in which the material has attained the optimum state for resisting the load, and in the tertiary stage the material has lost the ability to maintain this equilibrium condition and must yield at a greater rate to maintain integrity.

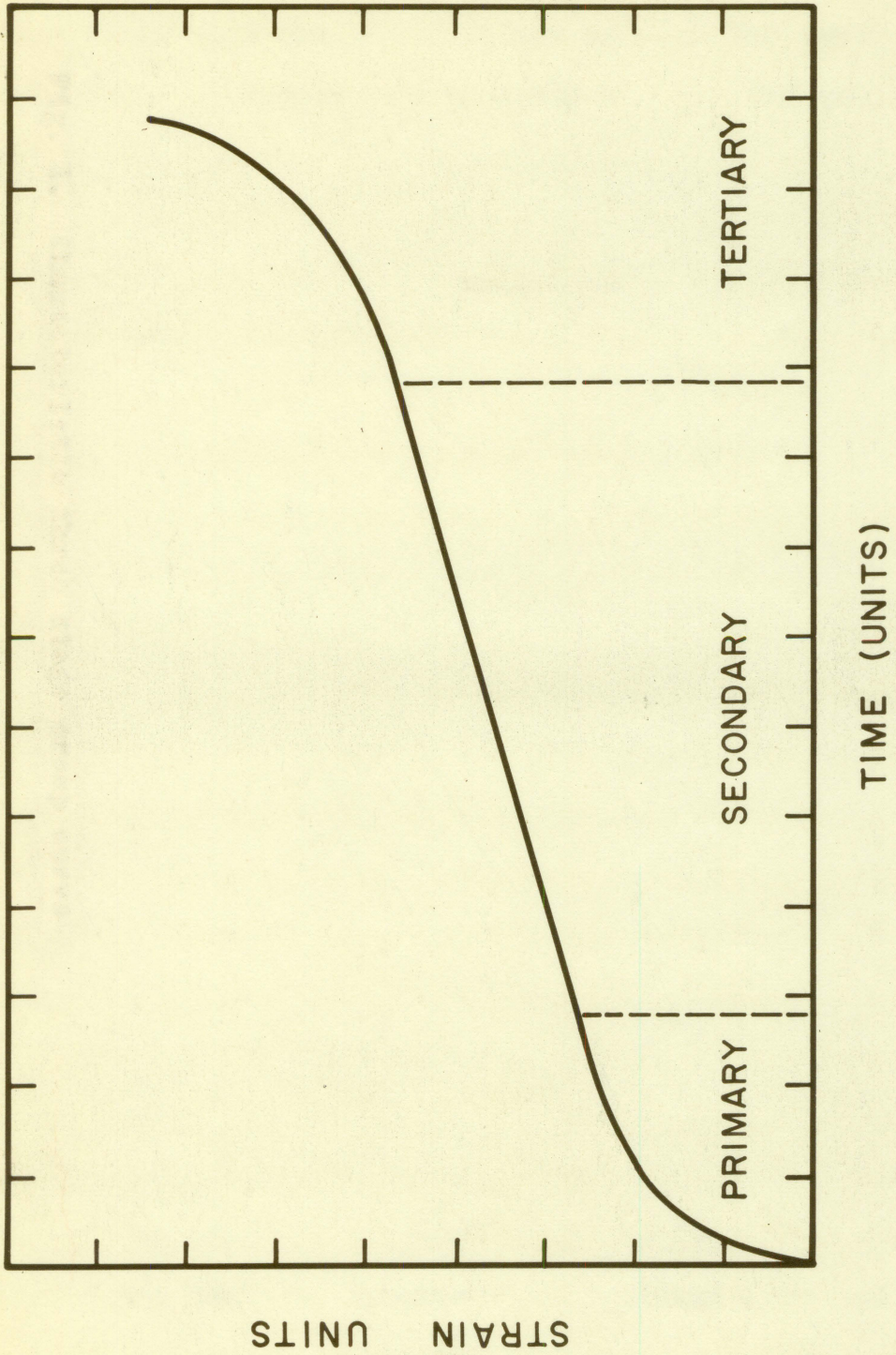


Fig. 1. Characteristic three stage creep curve

Most investigations have dealt with the primary and secondary stages. This is a result of practical considerations since once the material has entered the tertiary stage, the strain-time relationship has limited engineering application.

In some materials a second stage of creep does not appear and the creep curve reflects the initially decreasing strain rate followed by an increasing strain rate where the two regions are separated by a point of inflection.

Included in mathematical representations of the creep curve are stress, temperature, time and material parameters. It is in the choice of the latter that differences occur. The form of the equation is guided by theoretical considerations, dimensional analysis, and the experimental results. Since creep is dependent on material parameters, a mechanical equation of state involving only the external variables cannot truly describe the phenomenon, although under some conditions the application of such an equation has proven adequate.

1. Constant temperature conditions

With only a few exceptions, creep tests have been conducted under constant temperature conditions. Theoretically, this implies that the temperature condition does not vary

from the desired level, but from a practical standpoint an absolutely constant temperature test does not exist.

Sherby et al. (3) has postulated that in the absence of some thermal fluctuations, creep could not occur.

2. Cyclic temperature conditions

The introduction of a programmed temperature variation as one of the controlled variables provides a means of studying its effect on the strain history when compared to that resulting from a constant temperature test. Since there is no standard cyclic temperature test, considerable latitude exists as to the type of temperature variation which can be used.

A limited amount of testing has been accomplished under cyclic temperature conditions. The results, which have been summarized by Manson et al. (4), indicate that cyclic temperatures can have a large effect on the creep rate. The magnitude of the effect appears to be dependent on the material, shape of the specimen, severity of the thermal variation and the temperature level. If metallurgical changes occur due to the temperature variation or if severe thermal stresses are developed, the creep rate will reflect a very large change.

As a result of the cyclic temperature testing which has been accomplished, a number of mechanisms have been offered

to explain the results obtained. Because of the applicability to this investigation, a brief summary of these mechanisms will be presented.

Transient plastic deformation: (4) (5) (6) (7) (8)

According to the theory of nucleation, plastic flow occurs by the formation and growth of embryo slip bands. The growth of the slip band is relatively slow until a critical size is reached after which the growth continues rapidly and adds to the total strain. Under the conditions of constant stress and temperature a given rate of slip band nucleation and strain is attained. If either the stress or temperature is suddenly increased, a portion of the sub-critical slip bands become critical and grow. The strain rate initially becomes very high but then approaches the characteristic rate for the higher temperature or stress as the excess critical embryos become exhausted. If the stress or temperature is lowered, the critical size for slip band growth becomes larger than the existing embryos, and the strain rate becomes zero until new embryos can grow to the necessary critical size. Experiments conducted by Turnbull and Fisher (7), where temperature variations were applied, substantiated such a concept. It was noted in many instances the net creep occurring during a temperature cycle was greater

than if the maximum temperature had existed for the entire interval.

Aging and over-aging: (4)

The presence of finely dispersed precipitated particles provide the strength and creep resistance for many materials. Any change in the number, size or shape may therefore alter its mechanical properties. If the particles agglomerate to produce a size larger than the optimum, the hardness and creep resistance will decrease. The latter mechanism is termed over-aging. Often aging accompanies materials throughout their service life at elevated temperatures. Such aging can be either beneficial or detrimental. The rate of aging is considered to be an exponential function of temperature.

Solution and reprecipitation: (9) (10)

The solution of carbide particles in Ni-Cr steels at the high temperature and subsequent reprecipitation of larger particles upon cooling was observed by Avery and offered as the explanation for a resulting creep rate of 10 times or greater than that obtained with steady state conditions.

Internal inhomogeneity:

Boas and Honeycombe (11) report that temperature cycling in the absence of an external load on polycrystalline zinc,

cadmium, and tin caused plastic flow, grain growth and recrystallization. It was concluded such metallurgical changes could alter the creep behavior.

Embrittlement: (4)

A reduction in ductility due to metallurgical changes can occur and may be accelerated by cyclic temperature conditions. The form of the failure in this case is not considered true plastic flow since the failure and observed creep rate are the result of an early formation of internal micro-cracks. Generally embrittlement produces failure at a lower total elongation.

Dynamic effects:

The rate of achieving a given strain in a specimen can produce a subsequent effect of the remaining resistance to creep. Lequear and Lubahn (12) reported that a rapid rate of straining in Cr-Mo-V steel at 800°F produced a lower creep resistance than a more slowly strained specimen. Experiments of the same nature on aluminum at 78°K conducted by Tietz and Dorn (13) showed an opposite effect. While the two cases had conflicting results, the importance of strain rate history is quite apparent.

The importance of cyclic temperature conditions is best illustrated by noting some of the specific results obtained from the investigations which have been carried out. The

earliest investigation was conducted by Brophy and Furman (14) where non-constant temperature conditions were applied to 25-20 and 18-8 stainless steels. This work, reported in 1942 and subsequently verified by Avery and Matthews (10), showed a marked alteration of the strain history. The test temperature in the original work was varied from 1800°F through a series of lower temperatures and then raised back to the original temperature. Long periods were spent at each of the temperature levels and in a strict sense no repetitious temperature pattern was used. Large temperature increments were applied with rapid rates of heating and cooling. The strain rate obtained under the fluctuating temperature condition was 10 times that observed for the constant temperature test. Through the use of a thin tubular specimen it was demonstrated the acceleration effect in the solid specimen was due to thermal stresses as no acceleration of the creep was observed with the tubular specimen. Avery, in confirming the results of Brophy and Furman, used a temperature pattern of heating the specimen to 1800°F, holding it there for 20 hours and then allowing it to cool to room temperature in 24 hours. The creep rates were again much greater than with constant temperature tests, although in some cases a lower stress was used for the cyclic temperature tests. These results were explained on the basis of solution and reprecipitation of the carbides.

Guarnieri (15) using a similar temperature pattern in testing 321 stainless steel also found an accelerated creep condition. The effect was greatest at high temperature levels and increased with the length of time spent at the higher temperature. He attributed his results to thermal stresses and intergranular crack propagation.

The effect of cycling the temperature at a uniform rate about a mean test temperature is reported by Smith and Houston (16). Alloyed steels were tested about mean temperatures with a cyclic variation of $\pm 50^{\circ}\text{F}$. A comparison of the minimum creep rates for the cyclic temperature tests with the minimum creep rates obtained for constant temperature tests run at the average test temperature and the maximum temperature of the cycle showed in all cases the cyclic temperature creep rate to be greater than that obtained for the constant temperature condition.

Two analytical methods have been proposed for treating the problem of a non-steady temperature condition. The σ factor method was developed by Dorn and his co-workers (2) and will be dealt with more specifically under Analytical Relationships. It was originally intended to be applied to pure metals at temperatures above one-half the melting point on an absolute scale. If the creep curve for a given stress at one temperature is known, then the creep curves for all other temperatures at the same stress can be reasonably well

predicted. To accomplish this, strain is plotted against Θ , a temperature-compensated time.

$$\Theta = t e^{-\frac{\Delta H}{RT}} \quad \text{for constant temperatures}$$

t = test time

H = activation energy for creep

R = gas constant

T = absolute temperature

This approach is based on the premise that at a given strain a certain substructure of the material occurs regardless of the temperature at which the strain occurred.

The second analytical method is the Robinson Hypothesis, some times referred to as the Cumulative Creep Life. (4) (17) If a material is subjected to a stress and temperature for a given interval of time, then a particular fraction of its total life is used up. The creep curve under cyclic temperatures can be described by the summation of the portions of the total life used up at each of the temperature levels.

Both the Θ factor method and the Robinson Hypothesis have proven adequate in some instances in predicting cyclic temperature creep curves. If metallurgical changes occur as a result of the temperature variation, then neither method would be expected to be applicable.

B. Mechanical Properties of Tantalum

Tantalum, like some other materials, shows a wide variation in mechanical properties depending on the method of production, impurity content, and gaseous contamination during testing. For this reason the reporting of mechanical properties is usually accompanied by such details in order to allow comparison. Tantalum readily absorbs hydrogen, nitrogen and oxygen at elevated temperatures. The effects of such gaseous impurities, whether residual or obtained from contamination, has not been completely determined. Most of the known mechanical properties have been summarized in two reports prepared by Drennen et al. (18) and Ogden (19). At 1200°F, annealed arc cast tantalum was found to have a higher creep resistance than annealed sintered tantalum. The highest creep resistance was found in a fine grained sintered material which was degassed, cold rolled to 80% reduction and then recrystallized prior to testing. The lowest creep resistance was obtained for an extremely coarse grained thermally degassed material. Variation of the mechanical properties has also resulted from different shaped specimens being used. A comparison of room temperature tensile strengths given in Table 1 illustrates the variance encountered. The effect of oxygen contamination was determined by Glazier et al. (20). The ultimate tensile strength of tantalum at 4532°F, increased from 1730 psi to 3540 psi upon being contaminated with oxygen

Table 1. Room temperature tensile strength of tantalum (19)

Condition	Tensile strength psi
Recrystallized sheet ^a	67,140
Recrystallized rod ^b (annealed 1 hr at 1700°C)	49,800
Recrystallized rod ^c (annealed 1 hr at 2600°C)	33,500
Annealed sheet	40,000 to 50,000
Cold-worked sheet	100,000 to 200,000
Annealed high-purity sheet ^d (annealed 1 hr at 1200°C)	29,100

^aSupplied by Fansteel Metallurgical Corporation--
0.0056% N, 0.013% N, 0.02% C, 0.10% Cb, 0.01% W, 0.015% Fe.

^bSupplied by Fansteel Metallurgical Corporation--
0.01% N, 0.010% C.

^cFrom hydrogen-reduced powder--99.95% Ta, traces of Ni,
Fe, W, Cu, Ca, Si, Pb, Sn, Cr.

^dElectron-beam-melted tantalum supplied by Temescal
Metallurgical Corporation--0.0016% O, 0.0010% N, 0.00014% H,
0.0030% C, 0.0003% Cr, 0.01-0.03% Cb, 0.003% Cu, 0.0008% Fe,
0.0003% Ni.

during testing. From this it is seen that oxygen contami-
nation produced an appreciable strengthening of the material.

Murphy and Uhrig (21) have reported that at 800°C and
20 ksi the average value for the creep activation energy of

Pure sintered tantalum is 109,600 cal/gm-mole and the value of B , a stress parameter, is 5.65×10^{-4} in²/lb. They also point out that at 800°C the second stage creep is limited to short intervals of the test and is followed by an exponential stage in which both strain and strain rate vary exponentially with time.

III. OBJECTIVES OF THE INVESTIGATION

The investigations mentioned in Section II. have shown the marked effect of cyclic temperatures on the creep strength of certain materials. These investigations were conducted with large or relatively large temperature variations on materials which were subject to metallurgical changes.

This investigation was conducted to study the effect of cyclic temperatures of a small amplitude on a pure isotropic metal to minimize complicating factors. Any noticeable effect might thus be resolved on the basis of a particular structural change, or a basic mechanism of plastic deformation. The small temperature variation and slow rates of heating and cooling make the effects of thermal stresses negligible.

From an engineering standpoint, the application of the pure metal, such as tantalum, as the structural material for a reactor container or liquid-metal heat exchangers requires knowledge as to the effects of cyclic temperatures upon its creep properties. The development of a suitable testing facility was an integral part of the investigation and is also reported. Metallography of the material before and after testing is necessary to determine structural changes.

IV. ANALYTICAL RELATIONSHIPS

If creep is considered a time-rate phenomenon in which deformation occurs by movement of "flow-units" through a potential field with maxima and minima, then upon application of the load, dislocations are free to move until blocked by a barrier within the crystal. For the dislocation to proceed, it must be activated over the barrier or the barrier itself removed. At temperatures above one-half the melting point, Dorn (2) postulates the removal of the barriers to be the mechanism allowing the dislocations to progress. Atomic diffusion within the material controls the rate of removal of such barriers. Experimental evidence of Sherby and Dorn (22) supports this concept, where the activation energy for creep of many materials above one-half their melting temperatures is equal to that for self diffusion.

Based on such a concept a mathematical expression for the strain rate

$$\dot{\epsilon} = K'e^{B\sigma} e^{-\frac{\Delta H}{RT}} \quad (1)$$

was developed by Dorn where

$\dot{\epsilon}$ = change in strain with respect to time

K' = structural parameter

e = natural logarithm

B = material stress parameter

σ = stress

ΔH = creep activation energy

R = gas constant

T = absolute temperature.

Furthermore Dorn (2) has found above one-half the melting temperature, ΔH is a constant independent of stress, strain, temperature, structural changes, grain size, cold working and minor alloying additions. B is insensitive to structural changes but does decrease upon alloying and coldworking. K' must therefore vary with strain and reflect the changes occurring in the material as creep progresses. For second stage creep K' becomes a constant, reflecting a uniform rate of structural change, and Eq. 1 can be solved for the linear strain-time relationship.

$$\epsilon_{2nd} = K'e^{B\sigma} e^{-\frac{\Delta H}{RT}} t + \epsilon_0 \quad (2)$$

To evaluate ΔH , a sudden temperature change is applied to a test in progress. The strain rate is measured immediately before and after the temperature change and substituted into Eq. 1. This gives two expressions for the strain rate as a function of temperature

$$\dot{\epsilon}_1 = K'e^{B\sigma} e^{-\frac{\Delta H}{RT_1}}$$

and

$$\dot{\epsilon}_2 = K' e^{B\sigma} e^{-\frac{\Delta H}{RT_2}}$$

which can be solved for ΔH .

$$\Delta H = \frac{R \ln \frac{\dot{\epsilon}_1}{\dot{\epsilon}_2}}{\left(\frac{1}{T_2} - \frac{1}{T_1}\right)} \quad \sigma \text{ const.} \quad (3)$$

It is assumed K' remains essentially unchanged in the short time interval involved if the temperature change is small.

The stress parameter B can be evaluated in a similar manner by applying a sudden stress change. In this case

$$\dot{\epsilon}_1 = K' e^{B\sigma_1} e^{-\frac{\Delta H}{RT}}$$

and

$$\dot{\epsilon}_2 = K' e^{B\sigma_2} e^{-\frac{\Delta H}{RT}}$$

which can be solved for B .

$$B = \ln \frac{\dot{\epsilon}_1}{\dot{\epsilon}_2} \left(\frac{1}{\sigma_1 - \sigma_2} \right) \quad T \text{ const.} \quad (4)$$

For the exponential stage of creep reported by Murphy and Uhrig (21) in which $K' = K_0 \epsilon$, Eq. 1 becomes

$$\dot{\epsilon} = K_0 \epsilon e^{B\sigma} e^{-\frac{\Delta H}{RT}} \quad (5)$$

and

$$\epsilon = \epsilon_0 K_0 e^{B\sigma} e^{-\frac{\Delta H}{RT}} t \quad (6)$$

Dorn (2) has rearranged Eq. 1 to give the Zener-Hollomon parameter Z as

$$Z = \dot{\epsilon}_{2nd} e^{\frac{\Delta H}{RT}} = K_0 e^{B\sigma} \quad (7)$$

An analogous parameter Y for the exponential stage of creep can be obtained from Eq. 5.

$$Y = \frac{\dot{\epsilon}}{\epsilon} \exp. e^{\frac{\Delta H}{RT}} = K_0 e^{B\sigma} \quad (8)$$

For a constant stress Z and Y must be constants independent of the temperature.

Once ΔH has been experimentally determined for a material and a single creep curve for a given stress and temperature obtained, a strain - Θ curve can be plotted, where Θ , a temperature compensated time, is defined

by Dorn as

$$\Theta = \int_0^t e^{-\frac{\Delta H}{RT}} dt = e^{-\frac{\Delta H}{RT}} t \quad T \text{ const.} \quad (9)$$

Predicted creep curves for a different temperature can be obtained by evaluating Θ for the new temperature; Θ having corresponding values of strain on the experimental $\epsilon - \Theta$ curve. The value of Θ must be graphically integrated for cyclic temperature tests.

V. MATERIAL

Tantalum in the form of 1/2 in. diameter rod procured from the Pansteel Metallurgical Corporation and the National Research Corporation was used in this investigation. In both instances the material was tested in the received condition.

The Pansteel tantalum was produced by powdered metal techniques receiving a sinter at approximately 0.650 sq. in. then being rod rolled and swaged to the final 1/2 in. diameter. Vacuum arc melting was used to produce the National Research Corporation tantalum. The resulting 3 in. diameter ingot was skinned and swaged to the 1/2 in. diameter. Neither rod received any anneal after working. Based on the reduction in diameters the amount of cold work present was 45% and 83% respectively. Rockwell A hardness measurements of the untested materials were 41.5 and 41.9 in the same order.

The impurity content of the two materials as received is given in Table II. Examination of the grain structure of the untested materials was made using 90H₂SO₄ - 10HF as an electrolytic etchant. Well defined grains were present in the Pansteel tantalum as shown in Fig. 2. The results of the cold working of the NRC tantalum are apparent in Fig. 3 where the heavy distortion of the material produced a fibrous structure. Macroscopic observation of this distortion was

Table 2. Impurity content untested material (ppm)

Element	NRC Ta ^a	Fansteel Ta ^b
O	60	165
N	15	66
H	not determined	3
C	10	not determined
Fe	30	PT ^c
Cr	10	-- ^d
Ni	12	--
Cu	50	PT
Nb	25	560
Si	63	PT
Al	54	--
Ti	10	20
Mo	25	--

^aAnalysis furnished by National Research Corporation.

^bAmes Laboratory analysis.

^cPaint trace.

^dNot detected.

possible along the longitudinal axis where a definite "candy-stripe" structure was visible. Fig. 4 shows a recrystallized

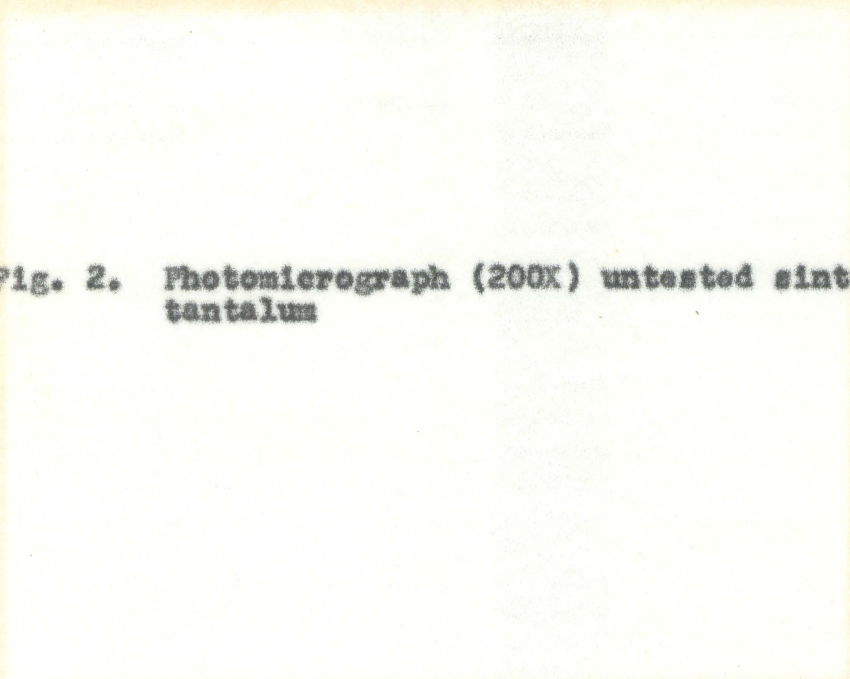


Fig. 2. Photomicrograph (200X) untested sintered tantalum

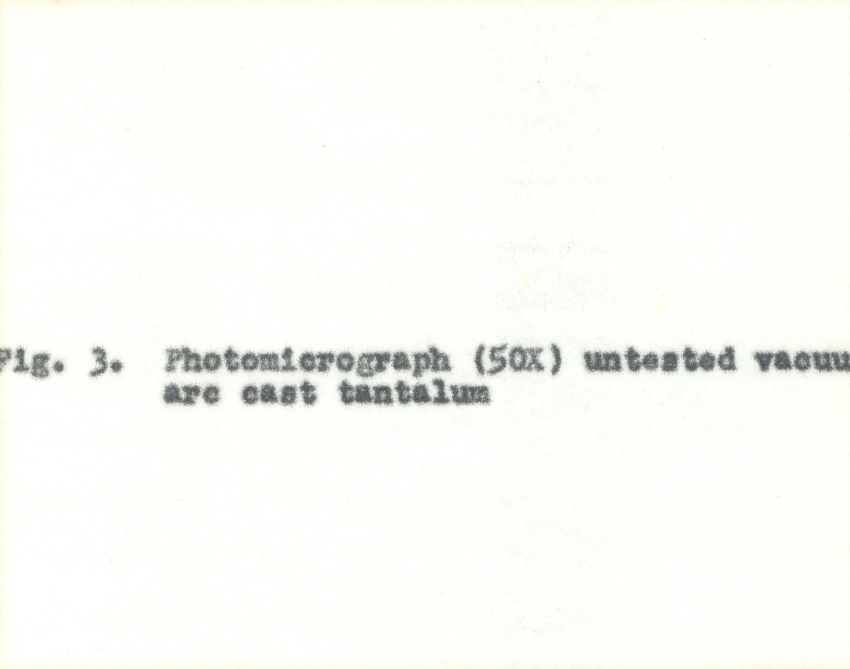


Fig. 3. Photomicrograph (50X) untested vacuum arc cast tantalum

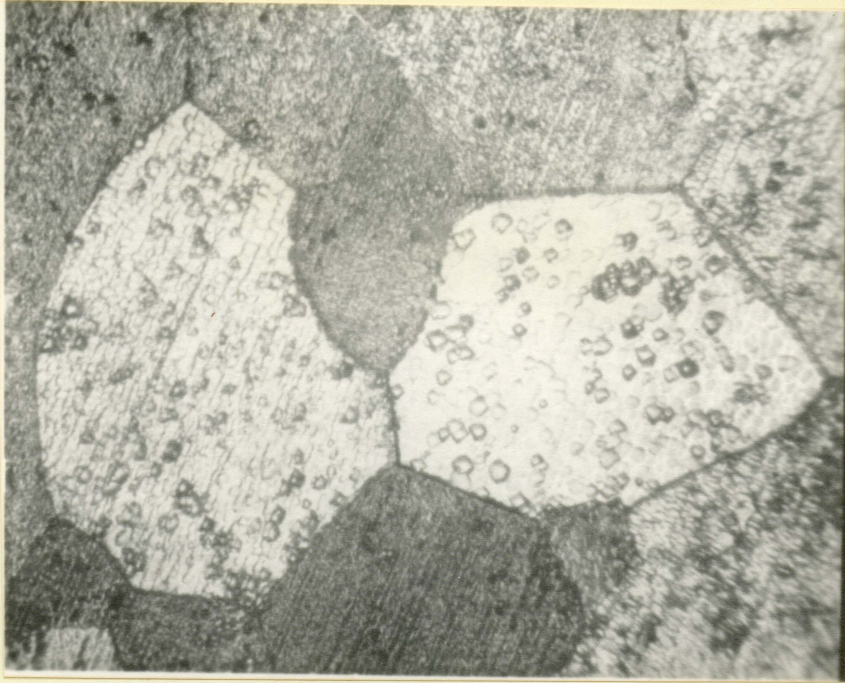
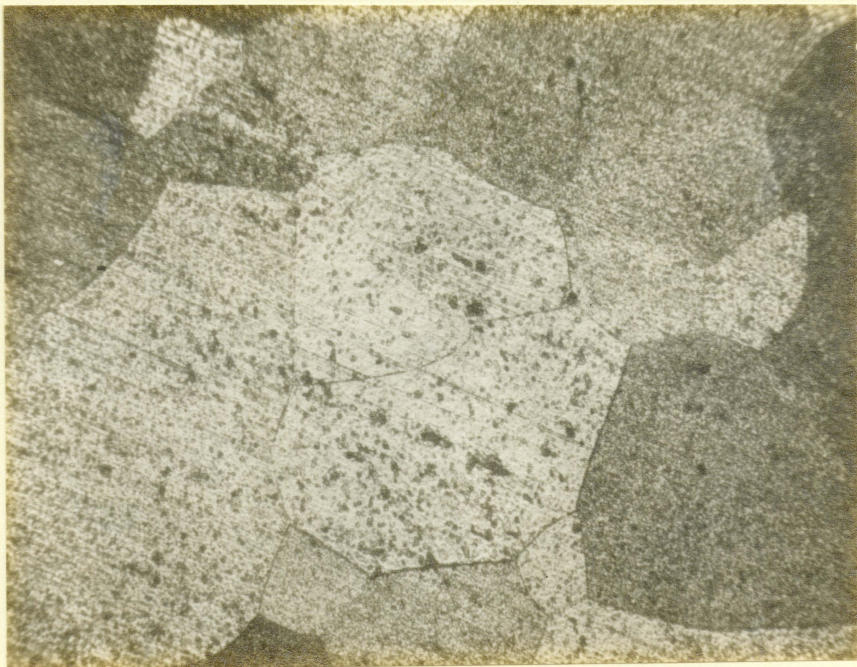


Fig. 4. Photomicrograph (200X) recrystallized
vacuum arc cast tantalum (annealed 1300°C)



sample of the NRC tantalum which had a Rockwell A hardness of 28.

Tantalum is a body centered cubic, isotropic material having no phase changes up to its melting point.

VI. EXPERIMENTAL PROCEDURES AND EQUIPMENT

Before a cyclic temperature investigation could be undertaken it was necessary to develop a suitable testing facility. As in any experimental investigation, the establishment of procedures was necessary to control the variables effecting the results. This section will therefore include a description of the equipment and the procedures followed in carrying out the investigation.

A. Testing Equipment

The problems normally associated with elevated temperature creep testing are obtaining accurate strain data, providing reliable temperature control and affording oxidation protection. To avoid the problems of training special personnel and the possible introduction of human error, a standard high temperature follow-up contact extensometer was used to measure the strain, with the measurement being autographically recorded on the same strip chart as the temperature. This greatly simplified the task of gathering the creep data, provided a continuous record of the strain and permitted ready inspection of the strain rate as the test progressed.

Because creep is highly temperature sensitive, precise temperature control is necessary. If small temperature variations can markedly alter the strain rate, a reliable and sensitive means of control must be provided over extended

periods of time. To permit the study of the effects of a small temperature variation, a controller was adapted to produce a desired programmed cyclic variation with the same degree of control. The desired temperature control was provided by an electronic proportioning controller (23) which utilized one leg of a Wheatstone bridge as the temperature sensing element.

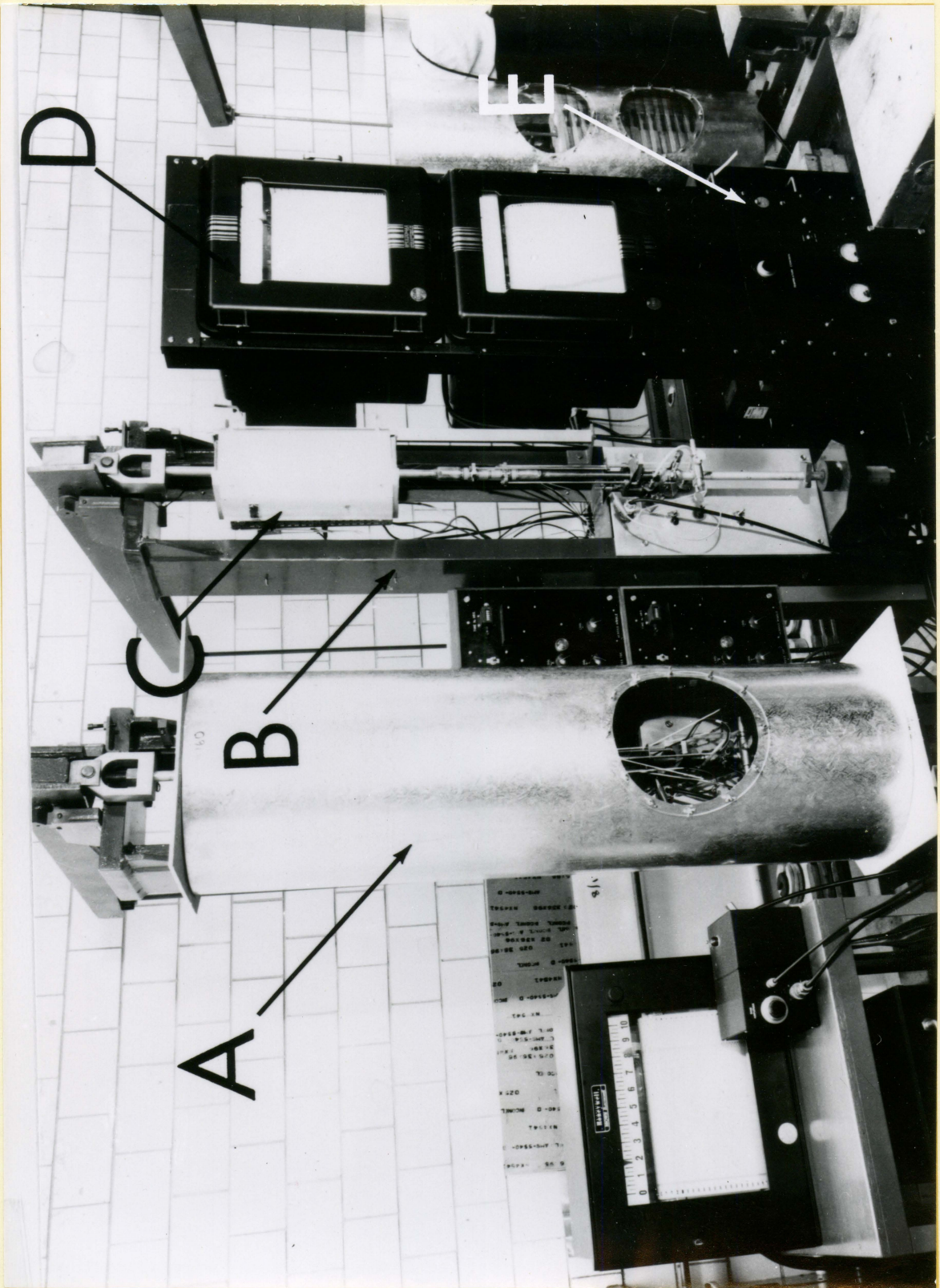
Oxidation protection was afforded by specimen encapsulation (24) which avoids the problems of large or cumbersome vacuum or inert gas systems and permits greater flexibility in the use of commercially available testing equipment.

Two test units were used for obtaining the creep data. A general view of these units is shown in Fig. 5. Each unit consists of a 12,000 lb lever arm creep machine, a two pen strip chart recorder, a multiple strip chart recorder, and an electronic proportioning furnace controller. These components provided the necessary systems for load application, strain measurement and recording, heating and temperature control, and temperature measurement and recording.

The protective hood shown in Fig. 5 on one of the creep machines prevented room temperature convection currents from affecting the furnace temperature and the extensometer. Prior to use of the hoods, the air currents disturbed the consistency of the strain measurement by causing irregular thermal variations.

Fig. 5. General view of creep facility

- A. Protective hood
- B. Creep machine
- C. Furnace
- D. Two-pen recorder
- E. Furnace controller



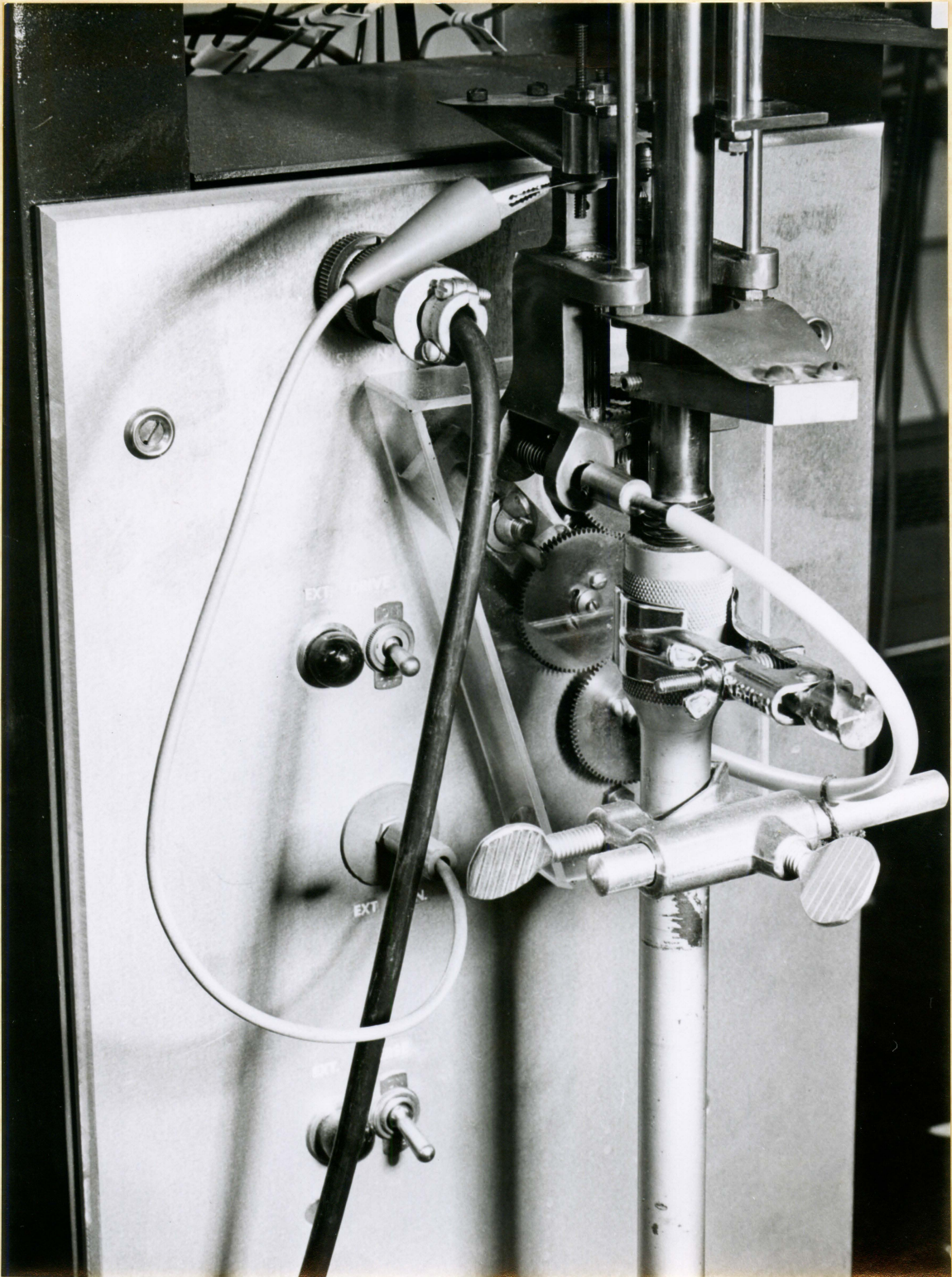
Load application:

The specimens were stressed by means of dead weights hung on the lever arms of the creep machines. A scissors type jack was used to support the weights and the lever arm while the temperature condition was achieved. Lowering of the jack provided a single, shock free loading within a few seconds. Prior straining of the specimen by the machine tare or incremental loading of the weights was thus avoided.

Strain measurement and recording:

The follow-up contact extensometer used to measure the strain is shown in Fig. 6. The extensometer attached to the shoulders of the specimen through two sets of contact points set a right angles to each other. To obtain a simultaneous autographic record of strain and temperature versus time, both quantities were transmitted to a two pen strip chart recorder. One pen of the recorder utilized a standard potentiometer circuit to measure and record the test temperature from 0-1000°C on a time base of 2" per hour chart speed. The other pen was activated with the extensometer by means of a synchro transmitter-receiver system. The synchro transmitter was mechanically driven by the extensometer drive motor, the receiver replaced one of the balancing motors furnished with the recorder. A schematic wiring diagram of the synchro system is shown in Fig. 7. Relays, operated by pen limit

Fig. 6. Follow-up contact extensometer



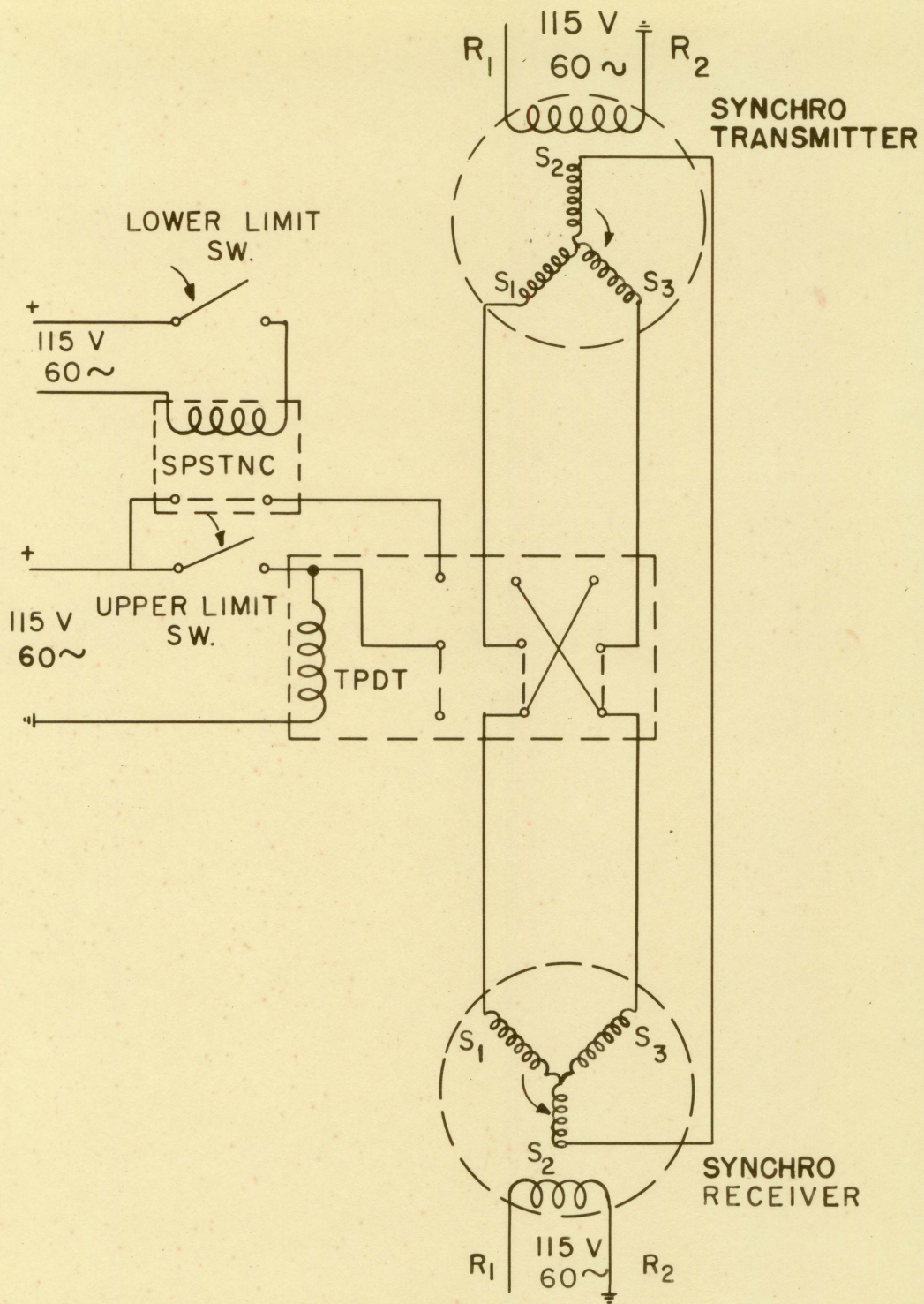


Fig. 7. Synchro system

switches, reversed the forward direction of the strain recording pen when either of the chart edges was reached. Fig. 8 shows the synchro receiver and pen limit switches mounted on the recorder.

Fig. 9 is a rear view of the creep machine front panel and Fig. 10 a schematic wiring diagram of those components except for the synchro transmitter. The extensometer reversing mechanism permitted the extensometer to follow the changes in length occurring in the extensometer rods and the specimen gage length resulting from cyclic temperature variations. Once a minute, for a period of 4 seconds, the reversing mechanism activated to drive the extensometer contact downward until contact was broken. Upon return to the forward direction, the contact was driven upward to the closed position.

The mechanical gears connecting the extensometer drive motor and the synchro transmitter are shown in Fig. 11. In this investigation the gear ratio was 1:1 which gave a recording sensitivity at the recorder of 12.31 micro inches/inch for the smallest division of the chart paper. (1 division = 1/10 inch or 10°C on the chart paper.)

Heating and temperature control:

Marshall vertical tube furnaces were used to heat the specimens, where the temperature distribution along the heat

FIG. 6. Two pen recorder

- A. Synchro receiver
- B. Balancing motor
- C. Pen limit switches

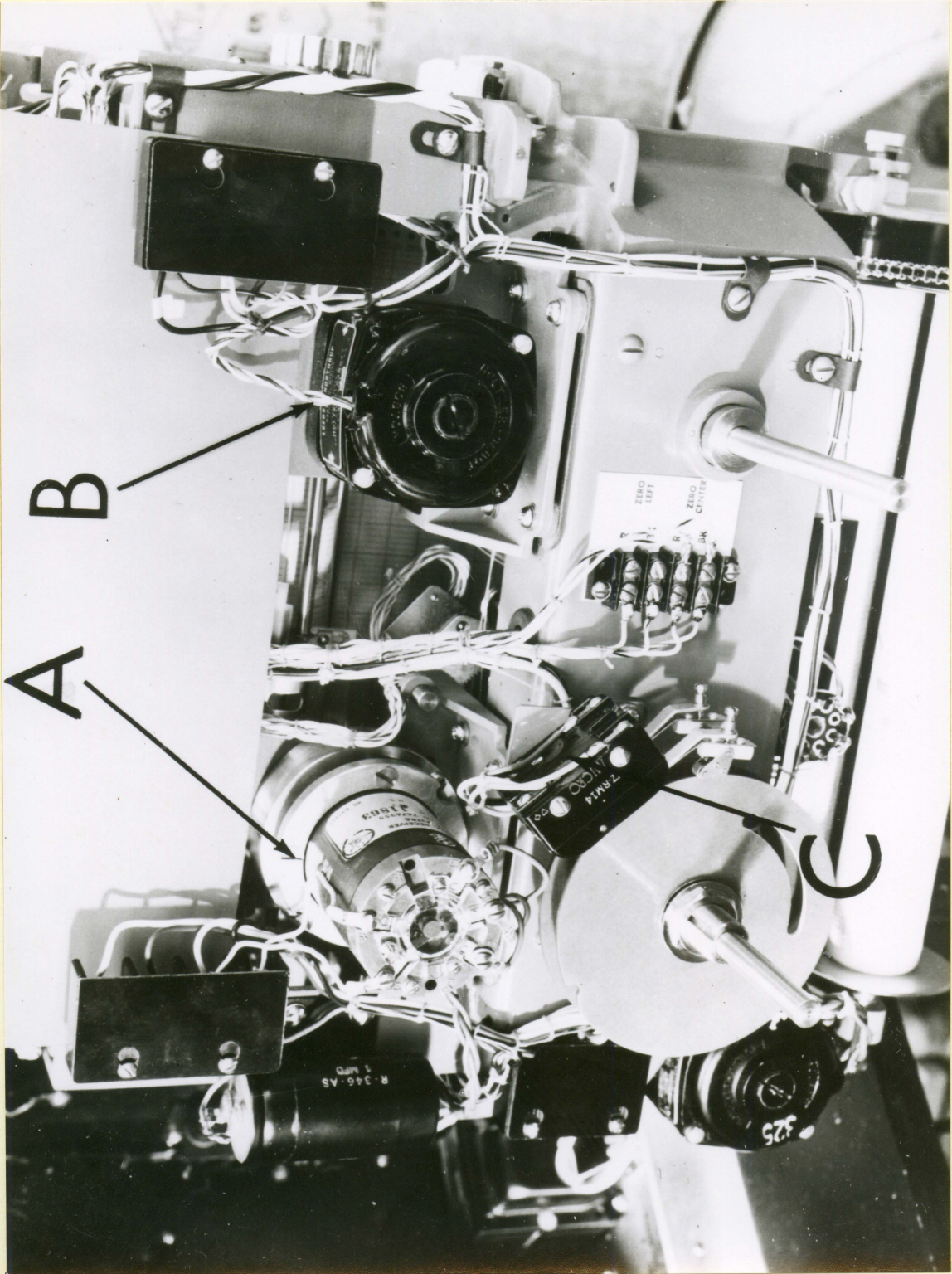
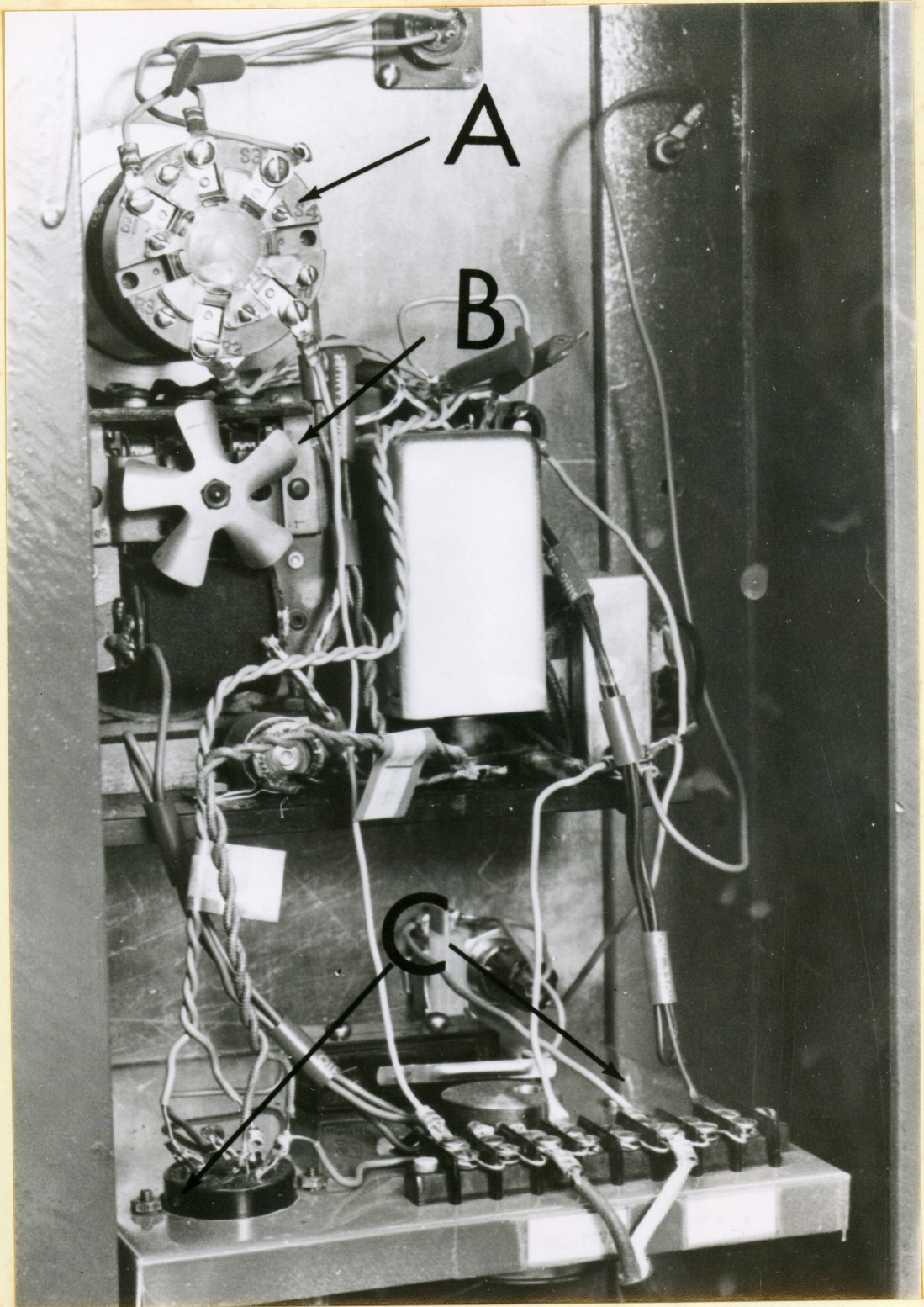


Fig. 9. Creep machine front panel (rear view)

- A. Synchro transmitter**
- B. Extensometer drive motor**
- C. Extensometer reversing mechanism**



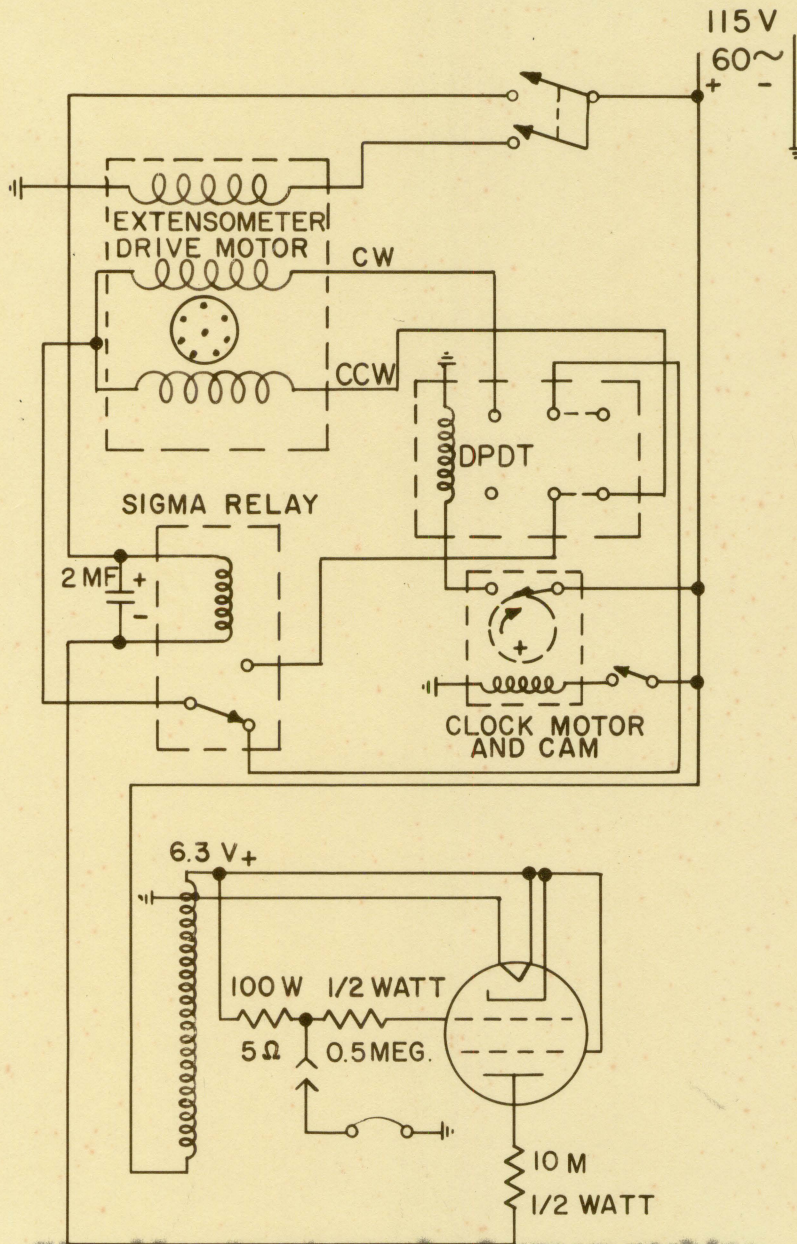
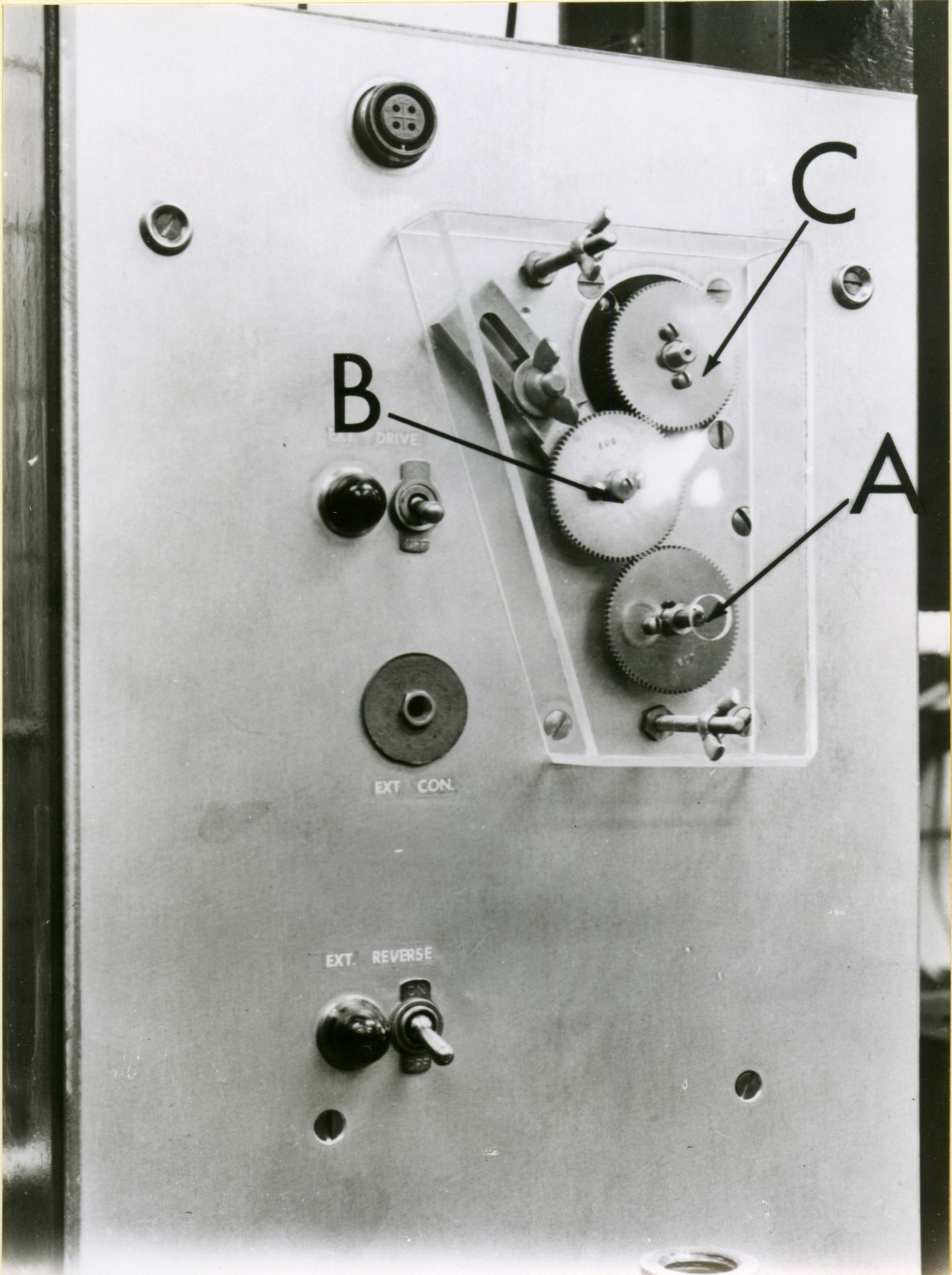


Fig. 10. Front panel of creep machine

Fig. 11. Gear train

- A. Extensometer drive motor shaft and gear
- B. Adjustable idler gear
- C. Synchro transmitter shaft and gear



zone was adjusted by means of variable resistors in parallel with the furnace windings. A platinum resistance thermometer, wound in close proximity with the middle furnace winding, served as the controller sensing element.

Electronic proportioning temperature controllers capable of maintaining a constant temperature condition to within $\pm 0.01^{\circ}\text{C}$ were designed and constructed by the Electronics Shop of the Ames Laboratory (23). In this application the variation of the specimen temperature did not exceed $\pm 1^{\circ}\text{C}$ from the desired condition.

A block diagram of the heating system is shown in Fig. 12. The resistance thermometer (RT) is one leg of a Wheatstone bridge circuit. A stabilized oscillator provides the bridge current. A signal due to bridge unbalance is fed to a high gain, narrow-band amplifier and then to a phase sensitive detector which controls the dc power amplifier. The dc amplifier regulates the current in the dc winding of the saturable reactor core. The ac windings of the reactor are in series with the line and the furnace windings. The addition of a motor driven sine function potentiometer between the bridge and narrow band amplifier provides a programmed sinusoidal temperature variation.

Temperature measurement and recording:

Standard equipment and techniques were used to measure and record the temperatures. Chromel-alumel thermocouples

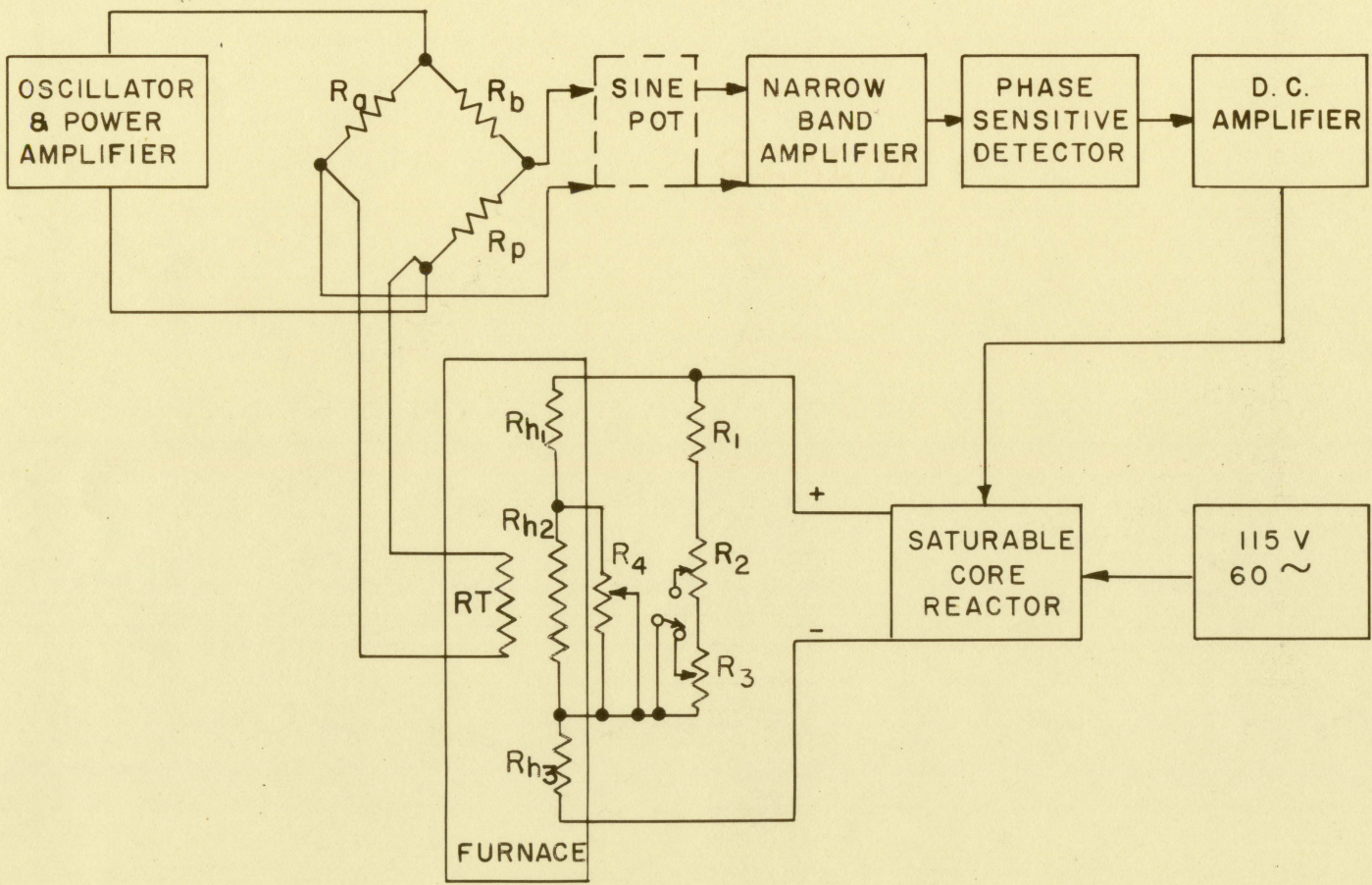


Fig. 12. Heating and temperature control system

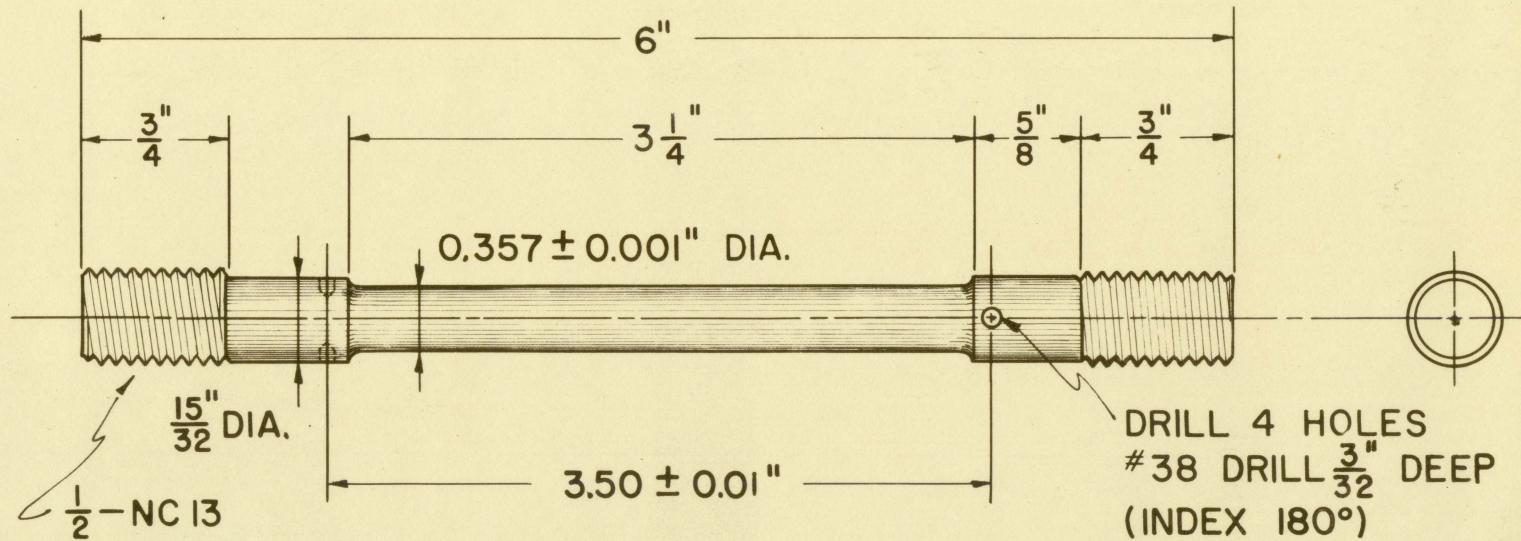
were employed exclusively. The test temperature was continuously recorded on the same time base as the strain record by the two pen recorders. To provide a means of determining the temperature distribution along the specimen, a multiple point recorder was used to measure and record the temperatures at six points along the specimen assembly.

B. Specimen Preparation

The 6-in. creep specimens shown in Fig. 13 were machined from 1/2-in. diameter tantalum rod. Following machining, the gage length of each specimen was polished with 600 grit silicon carbide paper to remove the machining marks. The specimens were washed in trichloroethylene and rinsed in alcohol to insure cleanliness prior to being encapsulated, the method used to afford oxidation protection.

Encapsulation of the specimens in small stainless capsules provides an oxygen tight barrier without encumbering other components of the testing facility. Application of this technique to creep specimens is reported by Bohn, et. al. (24). The outstanding advantages of this technique are its dependability with no maintenance, and allowing commercial high temperature testing equipment to be used.

Each capsule was fabricated from three sections of stainless steel bellows which were welded to machined



MACHINED FROM $\frac{1}{2}$ " DIAMETER RODS 6" LONG

CREEP SPECIMEN (F)

Fig. 13. Details of specimen

stainless steel fittings. The assembly of these components is shown in Fig. 14. A sectional drawing (Fig. 15) shows the functions of these components. Single ply, 5 mil seamless bellows were used, where minor forming operations on the end convolutions of each bellows were accomplished to match the corresponding weld flanges of the machined parts. Sealing of the assemblies was performed by shielded-arc welding in a specially designed unit shown in Fig. 16.

C. Discussion of the Variables Introduced by the Techniques

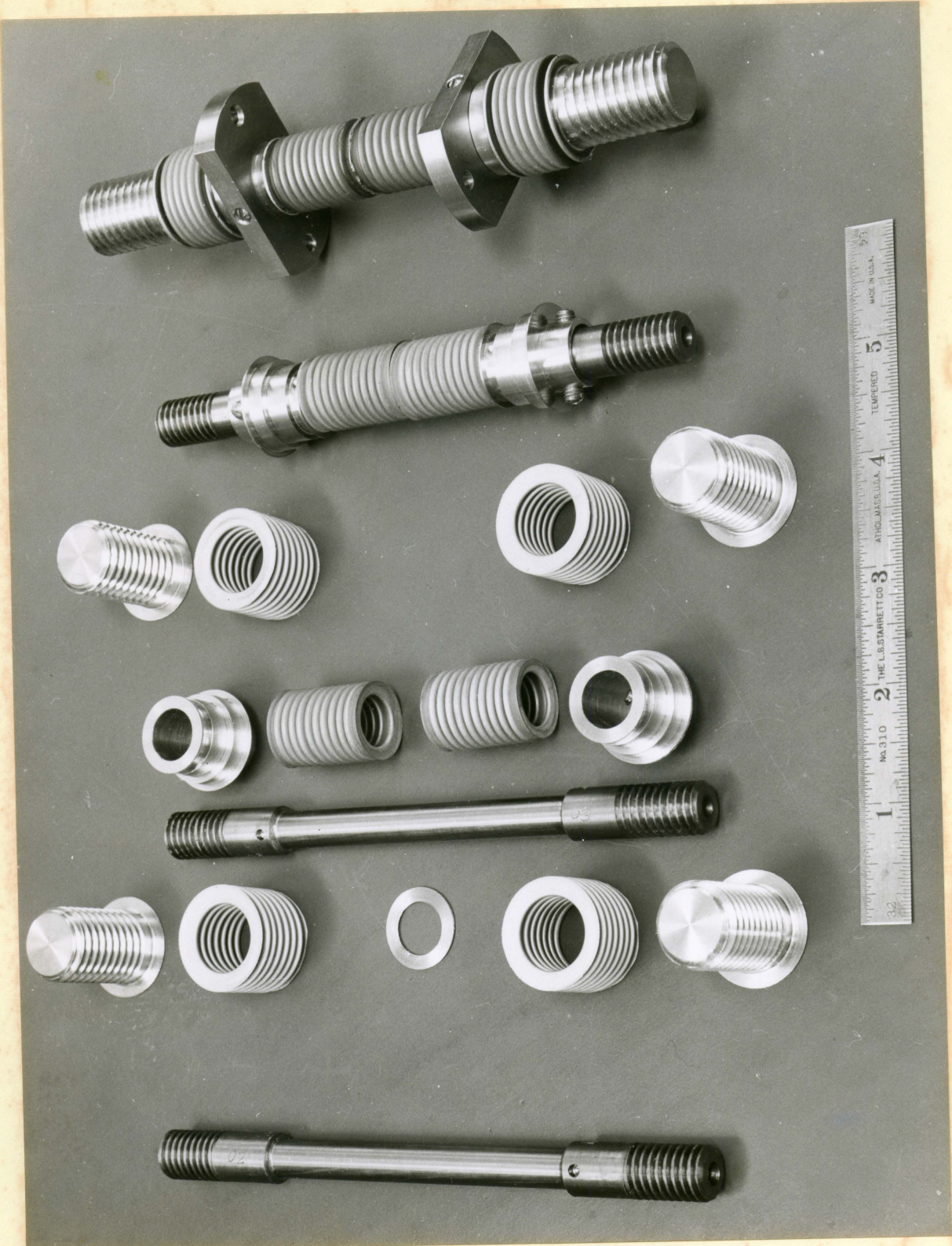
Material differences:

The two materials used in the investigation have been described in Section V. It would be expected the results obtained under identical testing conditions for each material would be different. Differences between specimens of each type were minimized by using material from a single rod in each case. Variations in the amount of cold working, impurity content and other fabrication variables are considered negligible.

Load application:

Variations in the rates of achieving the initial stress due to inconsistent loading techniques was avoided by use of the scissors jacks. The desired temperature condition was achieved under zero stress; after which, lowering the jack.

Fig. 14. Assembly of encapsulated specimen



- A. SPECIMEN END ADAPTERS
- B. END BELLOWS
- C. GAGE POINT FLANGE
- D. GAGE POINT MOUNTING RING
- E. CENTER BELLOWS
- F. CREEP SPECIMEN
- G. EXTENSOMETER RODS
- H. CREEP LOAD ROD

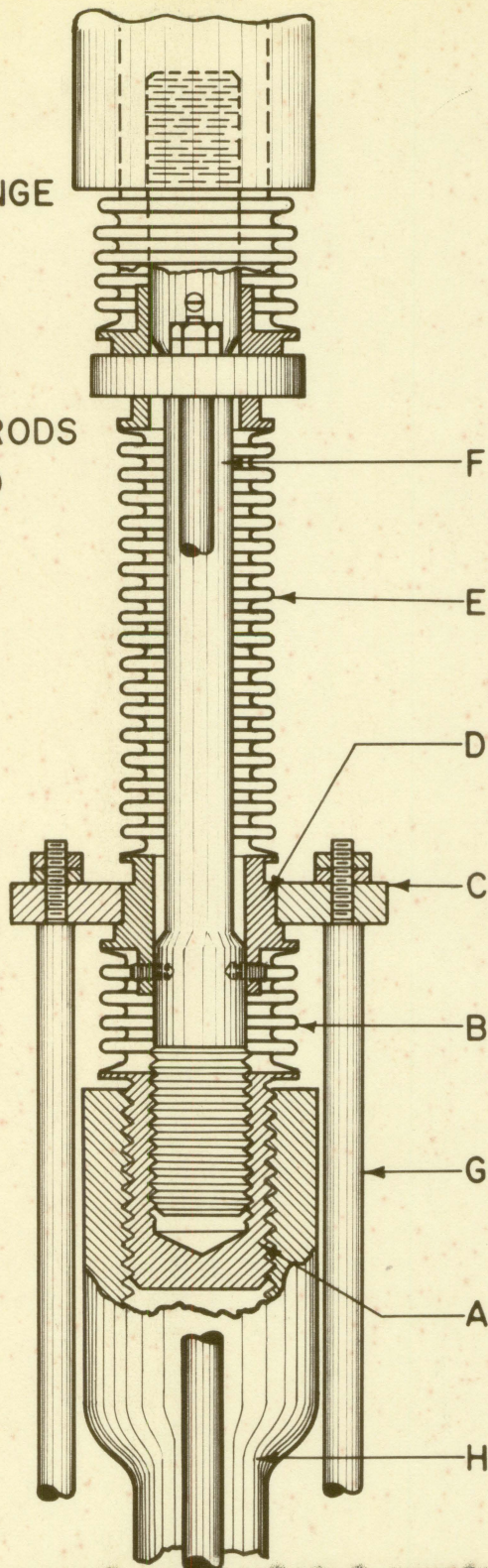
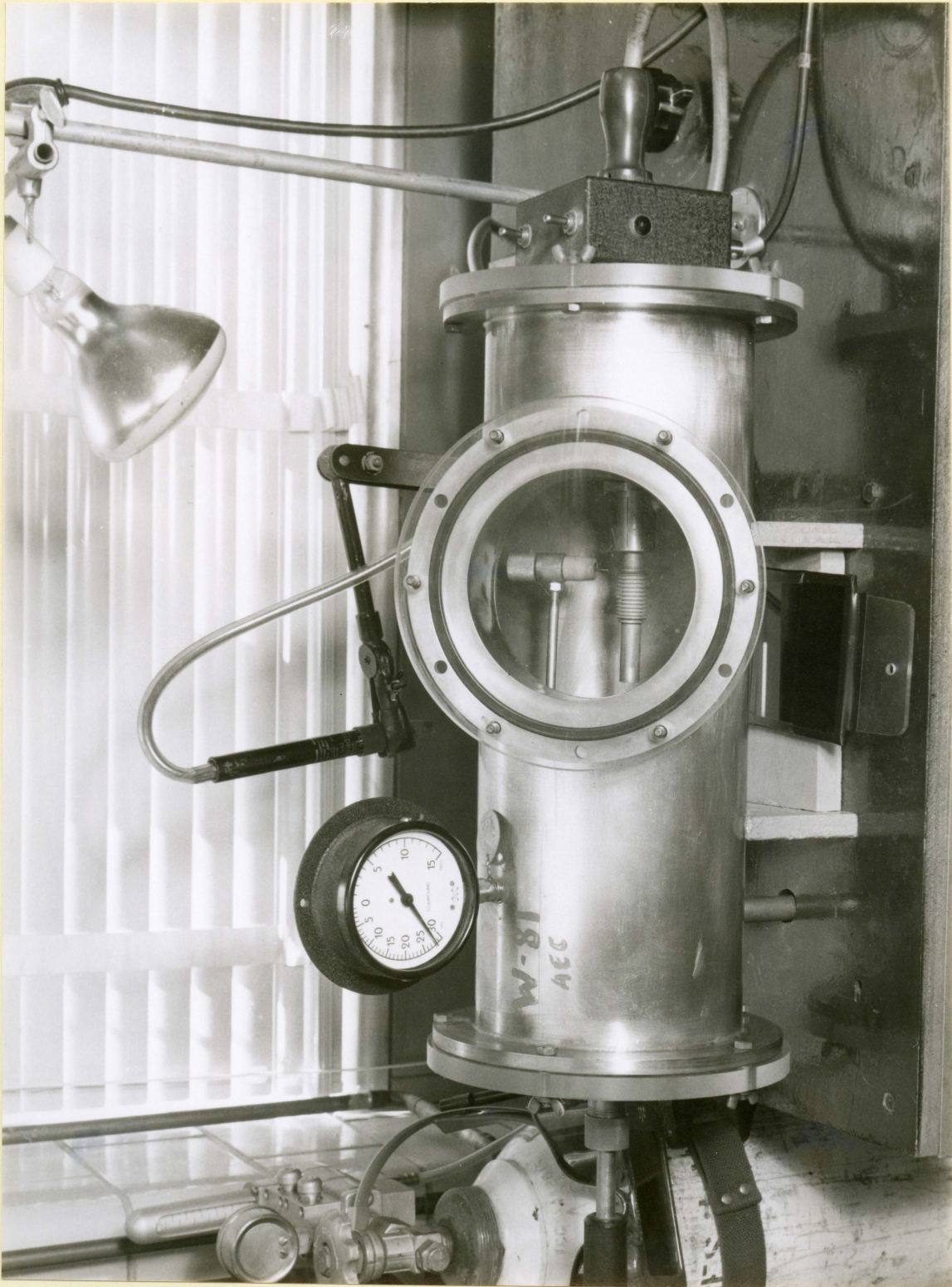


Fig. 15. Cross section of encapsulated specimen

Fig. 16. Welding chamber



applied the load in a smooth continuous manner within a time interval of a few seconds.

Stress variations:

Constant load creep machines were used in the investigation. When a localized reduction begins to occur prior to fracture, the effective stress begins to increase causing an acceleration of the strain rate.

Calculation of the load for each specimen was based on the diameter to the nearest 1/2 mil. This load was placed on the weight pan to the nearest 0.05 lb. Measurement of the specimen diameters was made with a machinists ball micrometer.

The creep machines were calibrated by the manufacturer to have less than 1% deviation from the true load. Variations of the relative initial stresses were less than 1/2%.

Temperature conditions:

The desired temperature condition was maintained to within $\pm 1^{\circ}\text{C}$. A continuous monitor of the temperatures was maintained throughout each test. Observation of the autographic strain record also provided a means of monitoring the temperature condition because the extensometer was sufficiently sensitive to thermal changes, to give an excellent index of the degree of temperature control.

The point of failure could conceivably be associated with a hot spot occurring in the 5°C vertical temperature

distribution. The use of the stainless assembly for oxidation protection precluded direct thermocouple readings of the specimen surface. It is not known what actual distribution occurred on the specimen, although it should not be greater than that observed on the outside of the assembly.

To determine what effect the encapsulation might have on the radial temperature distribution, a special assembly was fabricated in which a thermocouple was placed inside the stainless chamber to measure the specimen centerline temperature. With several determinations at the 800°C level, under both constant and cyclic conditions, the specimen centerline temperature always fell within the outside vertical distribution. The difference was attributed to radiation losses from the bellows and conduction losses of the specimen in the radial and vertical directions. With cyclic temperatures the vertical distribution remained relative; that is, both the outside bellows temperatures and the specimen temperature followed the applied variation. No discernable change in amplitude or phase was noted.

VII. RESULTS

A. Creep Curves

Composite creep curves for the two materials are shown in Figs. 17 and 18. Specimen 06 on Fig. 17 was tested at 800°C constant temperature and a stress of 21,000 psi. A comparison of the reduction in creep strength due to the introduction of a cyclic temperature condition is made on the basis of this test. The four cyclic temperature tests, 05, 07, 08 and 09, also shown on Fig. 17, were tested at 21,000 psi with an 800°C mean temperature. The temperature variations were applied sinusoidally at a frequency of one cycle per hour. From Fig. 17 it is seen that each of the cyclic temperature tests significantly weakened the material, the $\pm 5^\circ\text{C}$ test producing the greatest effect. Specimens 02 and 04 were both tested at 800°C constant temperature, but at lower stress levels. Specimen 04 was initially tested at 18,500 psi, and after creeping to 0.5% strain, the stress level was raised to 20,500 psi. Oxygen contamination during testing of specimens 02, 04 and 07 introduced an unanticipated variable in these three tests.

Specimen 11, on Fig. 18, was tested at 800°C constant temperature and 19,500 psi. At the same stress, specimen 10 was tested under cyclic temperature conditions at $\pm 5^\circ\text{C}$.

The NRC vacuum arc cast tantalum displayed four regions of creep: first, second, exponential and tertiary. The

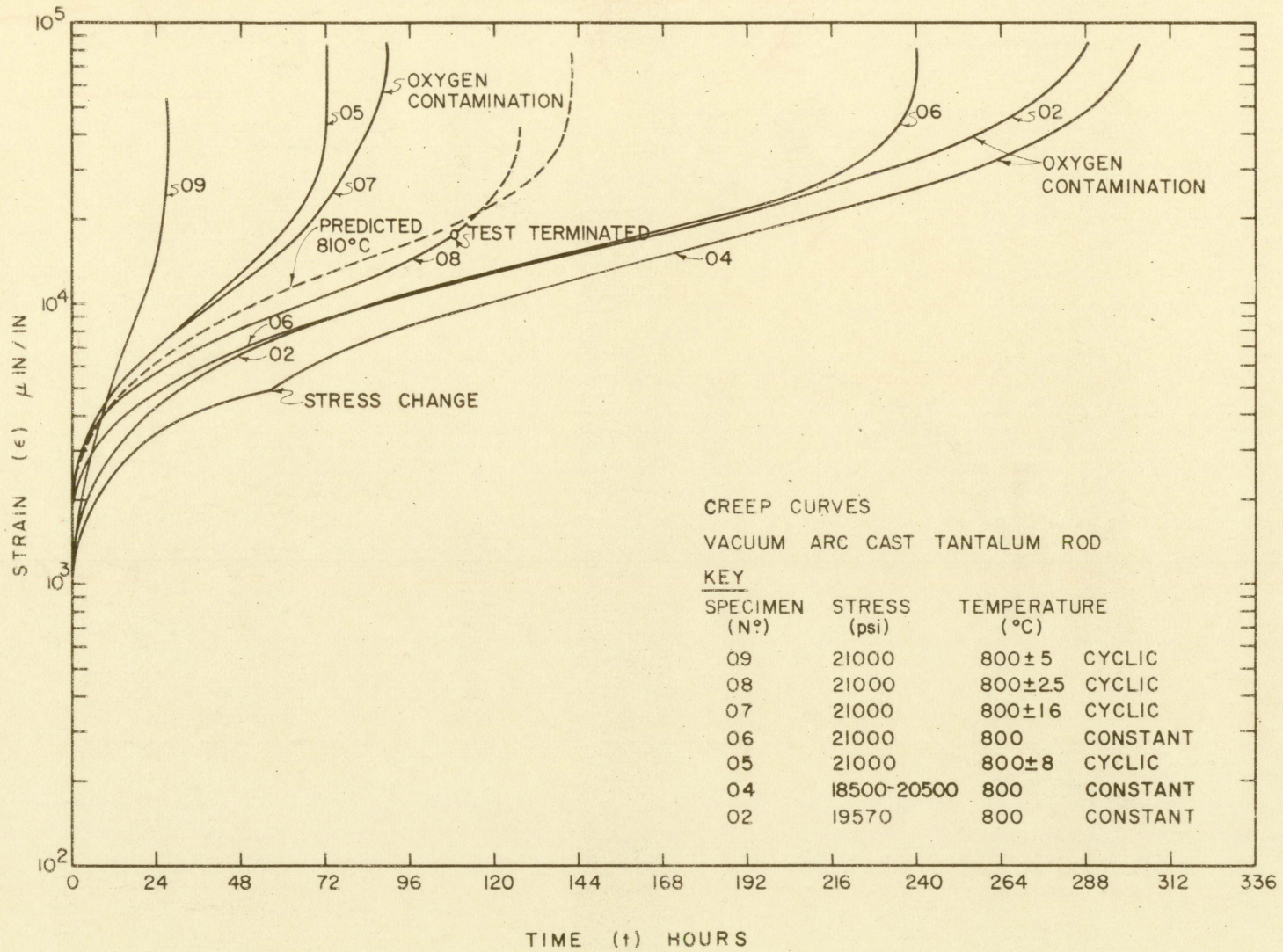


Fig. 17. Creep curves for vacuum arc cast tantalum

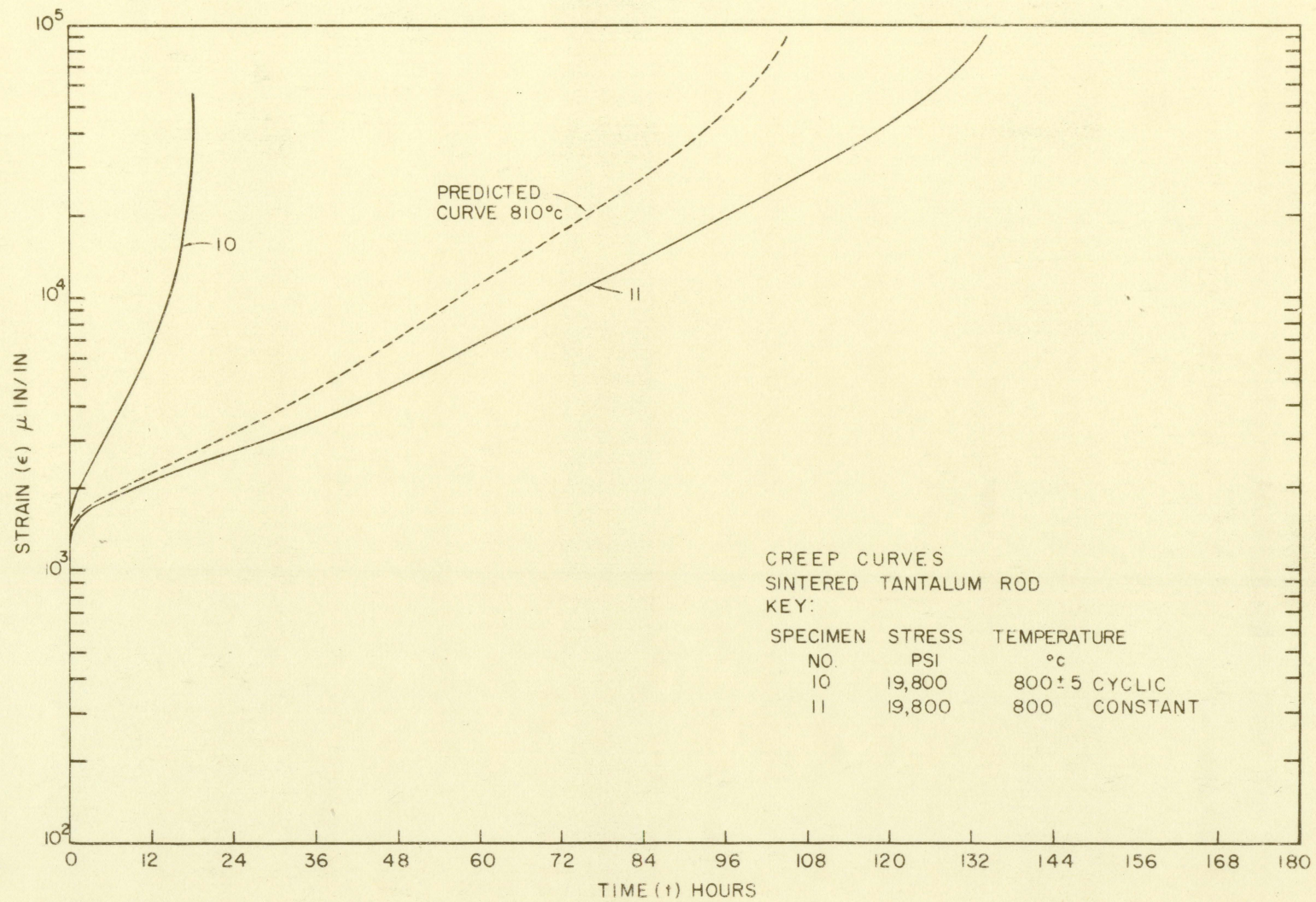


Fig. 13. Creep curves sintered tantalum

absence of second stage creep was noted for the Pansteel sintered tantalum. Pertinent information from the curves has been tabulated and presented in the next section in Table 4.

B. Evaluation of the Material Parameters

A single specimen NRC 03 was used to determine the values of ΔH and B. The temperature or stress was suddenly changed and the resulting change in strain-rate measured. Using Eq. 3 or 4 as appropriate, the values of ΔH and B were calculated. From a total of 16 temperature and 12 stress changes, average values of $115,925 \pm 2820$ cal/gm-mole for H and $(6.76 \pm 0.197) \times 10^{-4}$ in.²/lb for B were obtained. A tabulation of the determinations is given in Table 3. Within the temperature range of 780-825°C and stress level of 19,500 - 20,750 psi, both quantities were found to be independent of temperature, stress and strain.

Using the above values of ΔH and B for the NRC vacuum arc cast tantalum and the values reported by Murphy and Uhrig (21) for the Pansteel sintered tantalum; Z and K for second stage creep, and Y and K_0 for exponential creep were calculated for the various tests. It will be recalled

$$Z = \dot{\epsilon}_{2nd} e^{\frac{\Delta H}{RT}} = K_0 e^{B\sigma} \quad (7)$$

and

$$Y = \frac{\dot{\epsilon}}{\epsilon} \exp e^{\frac{\Delta H}{RT}} = K_0 e^{B\sigma} \quad (8)$$

Table 3. ΔH and B determinations

Determination	Temperature (°C) ^a		Stress (psi)		Elapsed Time (hr)	Accumulated Strain (in/in)	Strain Rate (in/in/hr)		ΔH (cal/gm-mole)	B (in ² /lb)x10 ⁻⁴
	Before	After	Before	After			Before	After		
ΔH_1	1073.5	1086.0	19,967	19,967	17.8	3564	72	130	115,700	—
ΔH_2	1086.0	1072.5	19,967	19,967	19.75	3766	130	68	113,200	—
ΔH_3	1072.5	1050.5	19,967	19,967	25.25	4080	68	37	119,500	—
ΔH_4	1050.5	1074.75	19,967	19,967	32.0	4622	37	78	118,000	—
B ₁	1074.75	1074.75	19,967	20,364	41.5	5121	49	64	—	6.6
B ₂	1074.75	1074.75	20,364	19,568	44.0	5275	64	37	—	6.9
B ₃	1074.75	1074.75	19,568	19,967	45.5	5318	37	49	—	7.22
ΔH_5	1072.75	1060.75	19,967	19,967	47.25	5386	80	43	114,600	—
B ₄	1060.75	1060.75	19,967	20,761	49.5	5466	43	74	—	6.77
ΔH_6	1062.5	1052.5	20,761	20,761	52.0	5856	74	43	119,300	—
ΔH_7	1054.25	1041.25	20,761	20,761	57.75	5884	37	18.5	116,400	—
ΔH_8	1041.25	1049.0	20,761	20,761	59.25	5908	18.5	33	115,800	—
ΔH_9	1049.75	1062.5	20,761	20,761	71.0	6198	31	62	120,000	—
ΔH_{10}	1063.0	1075.0	20,761	20,761	88.5	7017	37	68	115,000	—
ΔH_{11}	1072.25	1084.0	20,761	20,761	120	8839	49	89	115,800	—
ΔH_{12}	1085.5	1096.25	20,761	20,761	134.5	10,020	78	136	113,000	—
B ₅	1096.25	1096.25	20,761	20,364	137.0	10,340	130	99	—	6.87
B ₆	1096.25	1096.25	20,364	19,967	141.25	10,747	111	87	—	6.46
B ₇	1096.25	1096.25	19,967	19,568	147.0	11,288	89	68	—	6.77
ΔH_{13}	1095.0	1082.25	19,568	19,568	169.3	12,975	82	43	117,200	—
B ₈	1082.25	1082.25	19,568	19,967	182.5	13,781	62	40	—	6.55
B ₉	1082.25	1082.25	19,967	20,364	184.0	13,899	74	96	—	6.75
B ₁₀	1082.25	1082.25	20,364	20,761	189.0	14,378	96	130	—	6.86
ΔH_{14}	1083.5	1069.0	20,761	20,761	208.75	16,754	116	83	112,100	—
B ₁₁	1069.0	1069.0	20,761	19,967	214.25	17,246	83	49	—	6.55
ΔH_{15}	1071.0	1056.5	19,967	19,967	299.75	22,410	62	31	110,000	—
B ₁₂	1056.0	1056.5	19,967	20,761	323.25	23,097	68	117	—	6.84
ΔH_{16}	1059.0	1071.25	20,761	20,761	368.0	30,473	204	390	119,000	—

^aAverage of 6 values.

Table 4. Evaluation of terms

Specimen No. NRC	Stress (Ksi)	Temp (°K)	Stage	$\dot{\epsilon}_p$ (μ in/in/hr)	$\frac{\dot{\epsilon}}{\dot{\epsilon}_{exp}}$ (1/hr)	Elapsed Time (hrs)	Duration of 1st stage (hrs)	Duration of 2nd stage (hrs)	Duration exp. stage (hrs)	Duration tertiary stage (hrs)	Z ($\frac{1}{hr}$) $\times 10^{25}$	K ($\frac{1}{hr}$) $\times 10^{19}$	Y ($\frac{1}{hr}$) $\times 10^2$	K_0 ($\frac{1}{hr}$) $\times 10^{15}$	Rupture Time (hrs)	$\frac{\Delta H}{RT}$	σ_B	T^* (°K)
02	19.57	1073	2nd exp.	88.88	0.00711	30-95 95-195	30	65	100	93	3.65	6.64	2.845	5.15	288	2.5 $\times 10^{-24}$	5.5 $\times 10^5$	
03	19.97	1073	2nd	77.9		8-	8	complex temperature stress - history			3.16	4.34				2.5 $\times 10^{-24}$	7.29 $\times 10^5$	
04 04 04	18.5 20.5 20.5	1073	2nd. " exp.	48.5 80.65	0.01285	20- 60-116 116-240	20	56	124	63	1.94 3.25	7.18 3.25	5.1	4.9	302	2.5 $\times 10^{-24}$	2.7 $\times 10^5$ 1.042 $\times 10^6$	
05 05	21.0	1073	8 2nd. exp.	181.82	0.0252	8.5-26.5 26.5-51	8.5	18	24.5	22	7.15	4.89	9.925	6.79	72	2.5955 $\times 10^{-24}$	1.462 $\times 10^6$	1073.73
06 06	21.0	1073	2nd. exp.	85.47	0.00707	16-85 85-192	16	69	129	26	3.42	2.335	2.835	2.32	240	2.5 $\times 10^{-24}$	1.462 $\times 10^6$	
07 07	21.0	1073	16 2nd. exp.	170.94	0.0222	6.5-22.5 22.5-61	6.5	16.0	38.5	30	5.96	4.07	7.75	5.30	90	2.865 $\times 10^{-24}$	1.462 $\times 10^6$	1075.68
08 08	21.0	1073	2.5 2nd. exp.	106.4	0.0099	10-46 46-81	10	36	35		4.24	2.90	3.95	2.7	127est.	2.507 $\times 10^{-24}$	1.462 $\times 10^6$	1073.1
09 09	21.0	1073	5 2nd. exp.	317.5	0.077	3.5-9 9-17.5	3.5	5.5	8.5	9.5	12.5	8.54	30.3	20.7	27	2.54 $\times 10^{-24}$	1.462 $\times 10^6$	1073.36
FN 10 10	19.8	1073	5 exp.		0.1108	2-12	2	-	10	6			2.225	30.8	18	4.98 $\times 10^{-23}$	7.22 $\times 10^4$	1073.5
11 11	19.8	1073	exp.		0.0296	48-96			54	40			0.597	8.27	136	4.854 $\times 10^{-23}$	7.22 $\times 10^4$	

The values of the material parameters and other pertinent data from the experimental curves for each of the tests are tabulated in Table 4.

C. Application of the Θ Parameter

By definition

$$\Theta = \int_0^t e^{-\frac{\Delta H}{RT}} dt = e^{-\frac{\Delta H}{RT}} t \quad (9)$$

provided the temperature is constant. Using the latter form and the respective values of ΔH , ϵ versus Θ curves for the constant temperature tests, NRC 06 and Fansteel 11, are plotted on Fig. 19. From these curves, higher or lower temperature creep curves are predicted by evaluation of Θ for the new temperature. Cyclic temperature tests can also be predicted, where Θ must be evaluated by graphical integration to obtain a solution.

For a sinusoidal temperature variation

$$\Theta_{\text{cyclic}} = \int_0^t e^{-\frac{\Delta H}{R}} \left(\frac{1}{T_0 + A \sin \omega t} \right) dt = e^{-\frac{H}{RT'}} t$$

where T' is an equivalent constant temperature to produce the same value of Θ in one temperature cycle. As the cycle is repetitious, the value of T' is applicable throughout the

entire test. The values obtained for $e^{-\frac{\Delta H}{RT}}$ and T' by graphical integration of the cyclic temperatures are listed in Table 4. With the small temperature amplitudes used, the values of T' do not differ greatly from the average test temperature. Predicted creep curves, for T' equal to 1083°C , were obtained from Fig. 19, for both materials and are shown as the dashed curves on Figs. 17 and 18. It is apparent the experimental cyclic temperature creep curves can not be adequately described by the use of the Θ parameter. The values of equivalent temperature, T'' , necessary to normalize the experimental cyclic temperature curves to the respective constant temperature curves at 1% strain are listed in Table 5.

Table 5. Normalizing values of T''

Specimen	$\Delta T(^{\circ}\text{K})$	$T''(^{\circ}\text{K})$	$T'(^{\circ}\text{K})$
NRC 08	2.5	1078.1	1073.1
NRC 09	5.0	1102.62	1073.36
NRC 05	8.0	1088.35	1073.73
NRC 07	16.0	1087.84	1075.68
Fansteel 10	5.0	1107.65	1073.5

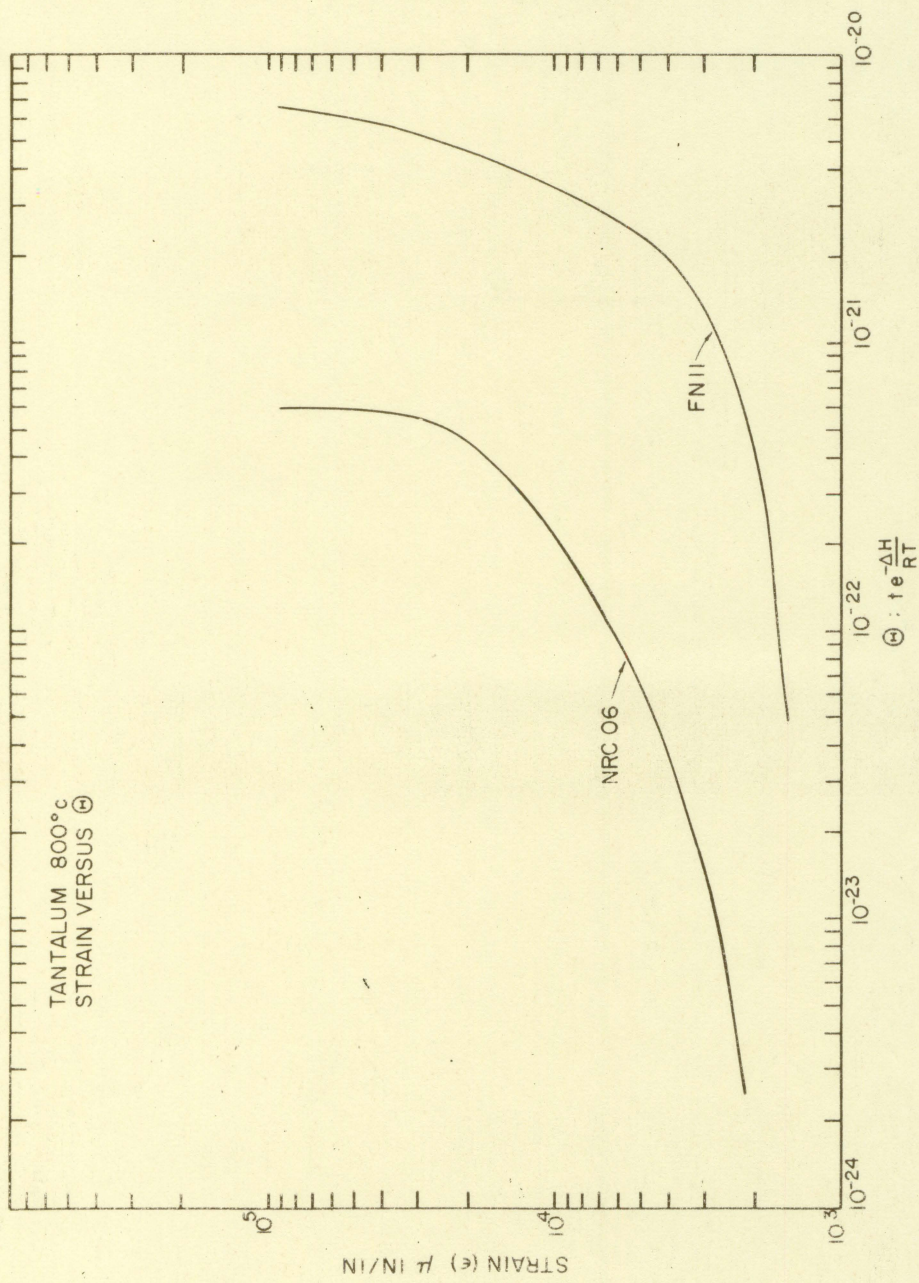


Fig. 19. Strain versus Θ curves

D. Metallography

Examination of the grain structure of each specimen after testing showed no apparent changes from the untested condition. In particular, evidence of recrystallization was sought in the more heavily worked vacuum arc cast material. Examples of the grain structure following testing are shown in Figs. 20 and 21.

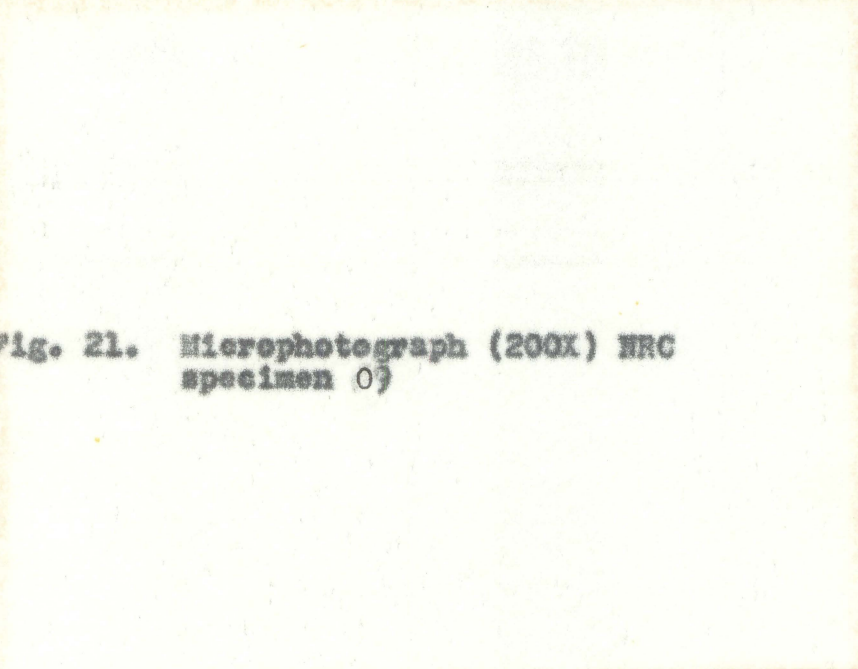
Samples of each tested specimen were analyzed for impurity content. The only significant change detected occurred in the gaseous impurities of the three contaminated specimens. The values of the gaseous impurities after testing are listed in Table 6.

Table 6. Gaseous impurity content (ppm)

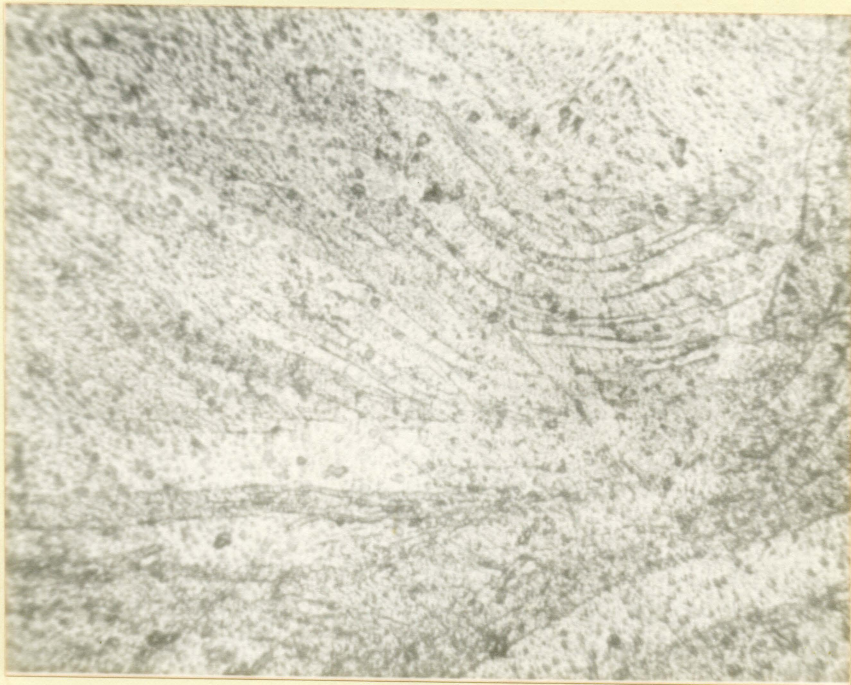
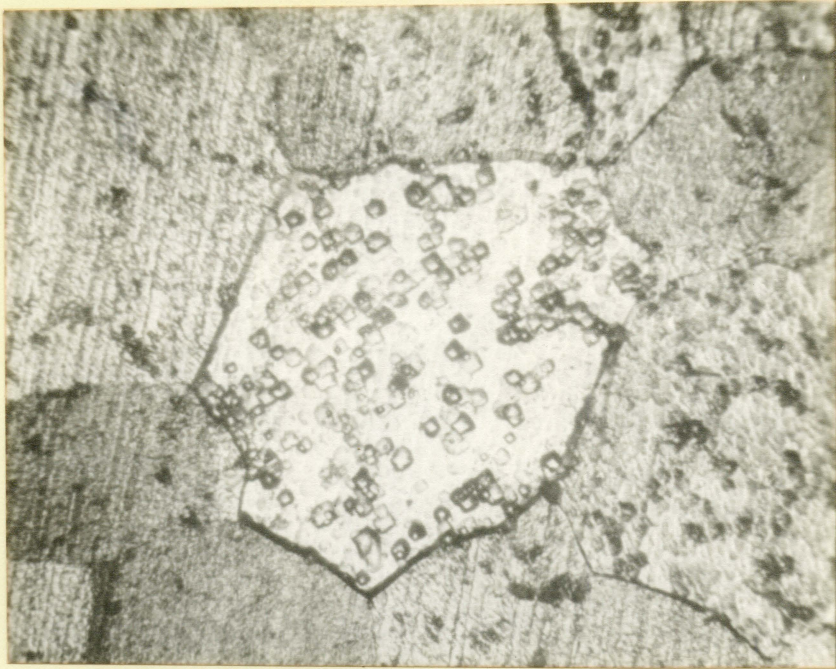
Material	Oxygen	Nitrogen	Hydrogen
untested NRC	95	2	5
untested Fansteel	165	66	3
Fansteel 10	184	78	3
Fansteel 11	113	55	4
NRC 02	130	170	2
NRC 03	92	8	4
NRC 04	2430	390	5
NRC 05	91	7	5
NRC 06	95	12	5
NRC 07	620	100	5
NRC 08	107	7	5
NRC 09	74	13	5



**Fig. 20. Microphotograph (200X) Fansteel
specimen #10**



**Fig. 21. Microphotograph (200X) HRC
specimen 09**



Average values of Rockwell A hardness determinations of the tested specimens are listed in Table 7. Oxygen contamination increased the hardness. Constant temperature testing of the vacuum arc cast tantalum did not alter the hardness, but cyclic temperatures produced a softening. A corresponding softening under cyclic temperature testing did not occur with the sintered tantalum.

Measurement of the specimen diameters along the gage lengths after testing showed a uniform reduction of a few 0.001 in. occurred except in the necked down regions of failure. The distorted grain structure in the vacuum arc cast tantalum produced a fibrous surface at the point of greatest reduction. The same region in the sintered material was characterized by an "orange-peel" surface. Figs. 22 and 23 show the fibrous and "orange peel" surfaces.

Specimen HRC 08, which was tested to approximately 1 1/2% strain, had begun to develop a region of localized reduction in cross-sectional area. The entire gage length was reduced 0.002 in. from the original diameter of 0.358 in. and the minimum diameter at the point of reduction was 0.350 in. The exponential stage of creep lasted until 1.3% total strain.

Table 7. Rockwell A hardness

Material	Hardness	Comments
Fansteel untested	42.5	
Fansteel 10	43.93	constant temperature
Fansteel 11	43.4	cyclic temperature
NRC untested	41.9	
NRC recrystallized	28.0	annealed 1300°C
NRC 02	49.2	constant temperature contaminated
NRC 03	38.41	complex stress and temperature history
NRC 04	45	constant temperature contaminated
NRC 05	33.1	cyclic temperature
NRC 06	41.86	constant temperature
NRC 07	41.5	cyclic temperature contaminated
NRC 08	34.5	cyclic temperature
NRC 09	34.35	cyclic temperature

Fig. 22. Reduced section NRC specimen 03
showing "fibrous" effect

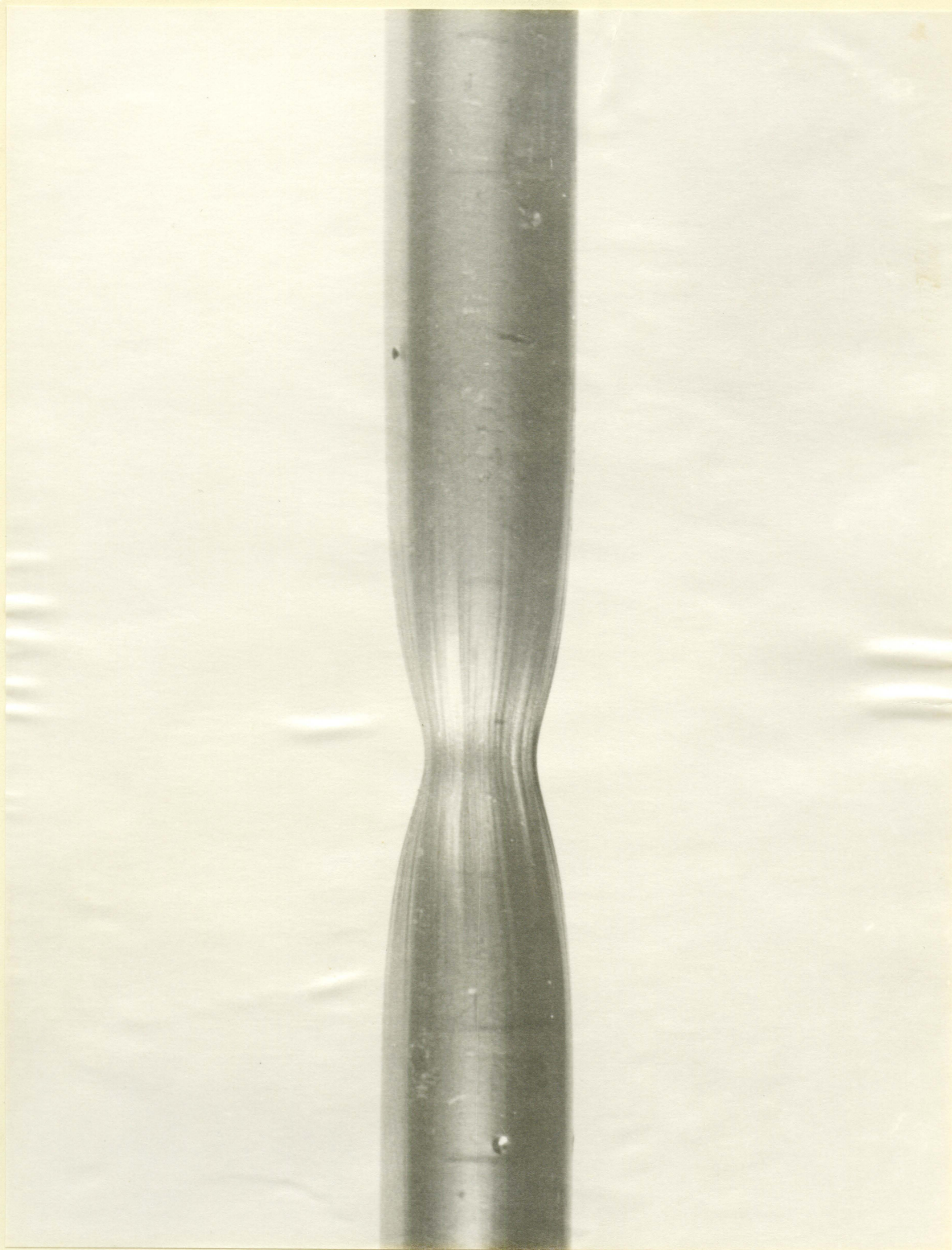
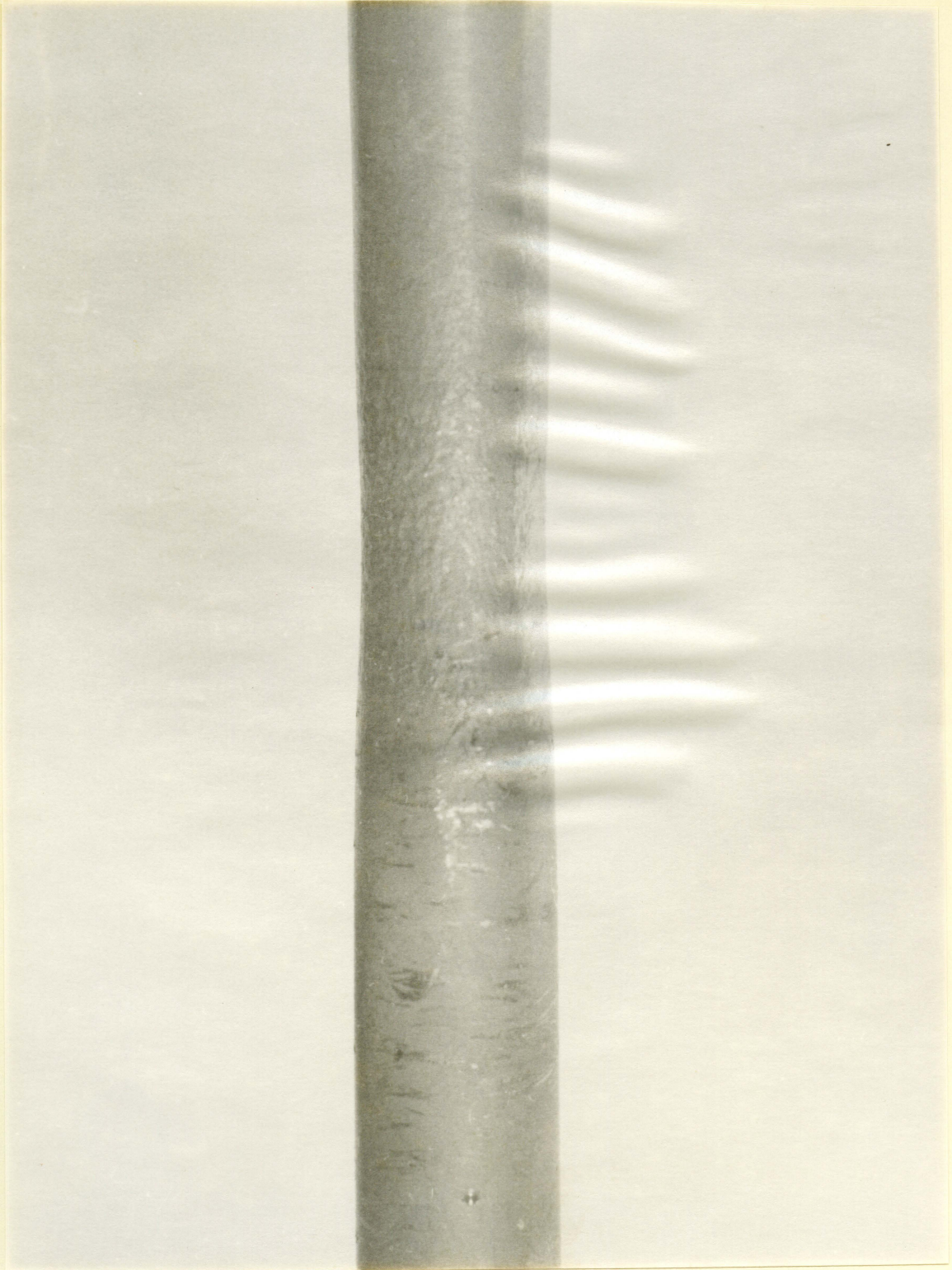


Fig. 23. Reduced section Pansteel specimen 11
showing "orange peel" effect



VIII. DISCUSSION AND CONCLUSIONS

The application of cyclic temperatures with small amplitudes, produced a marked reduction in the creep strength of both vacuum arc cast and sintered tantalum. The reduction in strengths was much greater than was predicted on the basis of the analytical technique. Depending upon the amplitude of the temperature variation, the decrease in rupture times varied to a factor of 1/2 to 1/9 of the constant temperature tests. The minimum creep rates obtained in the second stage for cyclic temperatures increased from the minimum creep rate for the constant temperature test by a factor of 1.3 to 3.8 and the ratio of $\frac{\dot{\epsilon}}{\epsilon}$ in the exponential stage by factors of 1.3 to 10.

Softening of the more heavily worked vacuum arc cast tantalum is indicative of a release of the strain produced by cold working. As the softening occurred only under cyclic temperatures, the change must be directly attributable to the dynamic temperature condition. Release of the strain due to cold working would allow the material to yield more readily to the applied load.

A corresponding softening under cyclic temperatures did not occur with the sintered tantalum. Yet the results of the $\pm 5^{\circ}\text{C}$ cyclic temperature on the creep strength in relation to its constant temperature test are in good agreement with

the results obtained for the vacuum arc cast tantalum. By way of comparison, the times for the $\pm 5^{\circ}\text{C}$ cyclic temperature tests to achieve 2% strain, are 13.25% and 17.8% of their respective constant temperature tests. The similarity of the results suggests that cyclic temperatures of small amplitudes enhances the mechanism of plastic deformation by more than one means. This would mean the release of the initial strain of cold working in the vacuum arc cast material was not the only accelerating effect. Discussion of the accelerating effect in terms of dislocation theory is not warranted.

The results of the four cyclic temperature tests on the vacuum arc cast tantalum do not vary consistently with the increasing temperature amplitude. Contamination of the $\pm 16^{\circ}$ test during testing, which would introduce interstitial atoms, should strengthen the material. This might explain why the resulting creep curve is quite similar to the $\pm 8^{\circ}\text{C}$ test. The combined effects of cyclic temperature softening and contamination hardening left the hardness unaltered in this instance.

The $\pm 5^{\circ}\text{C}$ test produced the greatest change in creep resistance for the vacuum arc cast tantalum. Provided the results of this single test are truly representative of that temperature condition, an optimum temperature variation for operation of the weakening mechanism or mechanisms exists.

The existance of such an optimum does not coincide with the present understanding of the mechanisms of plastic deformation.

The introduction of the unanticipated variable of contamination in three tests, resulted from pin hole leaks in the encapsulation assemblies.

Contamination did produce a notable change in the shape of the tertiary stage in all three instances. Other observations would be purely speculative, as the contributions of the other factors of stress level, stress change and temperature condition are not known.

IX. SUGGESTED TOPICS FOR FUTURE INVESTIGATION

A study of cyclic temperature effects on annealed tantalum will give a correlation between the magnitude of the effect in the presence and absence of cold working.

The effects of small cyclic temperatures, studied at other stress and temperature levels, and with various frequencies would provide a better understanding of this phenomenon. Such information is necessary before an adequate theory can be developed.

X. LITERATURE CITED

1. Fisher, R. W. and Fullhart, C. E. Feasibility studies on molten metal reactor components. Proceedings of the Second United Nations International Conference on the Peaceful Uses of Atomic Energy, Geneva, Paper 199. 1958.
2. Dorn, J. E. Creep of metals as a reaction-rate phenomenon. In Robertson, G. R., ed. Modern chemistry for the engineer and scientist. 276-297, New York, N. Y., McGraw-Hill Book Co., Inc. 1957.
3. Sherby, O. D., Lytton, J. L. and Dorn, J. E. Activation energies for creep of high purity aluminum. University of California, Minerals Research Laboratory, 46th technical report. 1956.
4. Hanson, S. S., Sachs, G. and Brown, W. F., Jr. Literature survey on the effect of cyclic heating and loading on the creep, stress-rupture and fatigue properties of metals at elevated temperatures. U. S. Atomic Energy Commission Report NP-6798. [Technical Information Service, AEC] 1957.
5. Fisher, J. C., Helleman, J. H. and Turnbull, D. Nucleation. Journal of Applied Physics. 19: 775-784. 1948.
6. Turnbull, D. and Fisher, J. C. Rate of nucleation in condensed systems. Trans. American Institute of Mining and Metallurgical Engineers. 175:774-785. 1949.
7. Turnbull, D. Transient nucleation. Trans. American Institute of Mining and Metallurgical Engineers. 17:71-73. 1948.
8. Carreker, R. P., Leschen, J. G. and Lubahn, J. D. Transient plastic deformation. Trans. American Institute of Mining and Metallurgical Engineers. 180:139-146. 1949.
9. Avery, H. S. Discussion of "Cyclic temperature acceleration of strain in heat resisting alloys." Trans. American Society for Metals. 30:1130-1133. 1942.

10. Avery, H. S. and Matthews, H. A. Cast heat resisting alloys of the 16% chromium, 35% nickel type. Trans. American Society for Metals. 38:957-1022. 1947.
11. Boas, W. and Honeycombe, R. W. K. Plastic deformation of non-cubic metals by heating and cooling. Proc. Royal Society of London. Series A, 186:57-71. 1946.
12. Lequear, H. A. and Lubahn, J. D. Effect of strain rate history on the creep behavior of an alloy steel at 800°F. Proc. American Society for Testing Materials. 55:719-723. 1955.
13. Tiets, T. E. and Dorn, J. E. Effect of strain histories on the work hardening of metals. American Society for Metals, Cold Working of Metals, 163-179. 1949.
14. Brophy, G. R. and Furman, D. E. Cyclic temperature acceleration of strain in heat resisting materials. Trans. American Society for Metals, 30:1115-1129. 1942.
15. Guarnieri, G. J. Creep-rupture properties of aircraft sheet alloys subjected to intermittent load and temperature. American Society for Testing Materials Special Technical Publication 165:105-148. 1954.
16. Smith, G. V. and Houston, E. G. Experiments on the effects of temperature and load changes on creep rupture of steels. American Society for Testing Materials Special Technical Publication 165:67-98. 1954.
17. Robinson, E. L. Effect of temperature variation on the creep strength of steel. Trans. American Society of Mechanical Engineers. 60:253-259. 1938.
18. Drennen, D. C., Langston, M. E., Slunder, C. J. and Dunleavy, J. G. High-temperature mechanical properties of tantalum. U. S. Atomic Energy Commission Report BHI-1326. [Battelle Memorial Institute, Columbus, Ohio] 1959.

19. Ogden, H. R. Physical and mechanical properties of tantalum. U. S. Atomic Energy Commission Report DMIC Memorandum 32. [Defense Metals Information Center, Battelle Memorial Institute, Columbus, Ohio] 1959.
20. Glazier, L. P., Jr., Allen, R. D. and Saldinger, I. L. Mechanical and physical properties of the refractory metals, tungsten, tantalum, and molybdenum, above 4000°F. Aerojet-General Corporation, Azusa, California. Report No. M1826. 1959.
21. Murphy, Glenn and Uhrig, R. E. Observations on the creep of tantalum. U. S. Atomic Energy Commission Report IS-66. [Iowa State University of Science and Technology] 1959.
22. Sherby, O. D. and Dorn, J. E. Correlations of high temperature creep data. University of California, Minerals Research Laboratory, 41st technical report. 1955.
23. Svec, H. J., Read, A. A. and Hilker, D. W. Proportioning furnace temperature controller. U. S. Atomic Energy Commission Report ISC-585. [Iowa State College] 1958.
24. Bohn, J. R., Uhrig, R. E. and Murphy, Glenn. Method of specimen corrosion protection for high temperature creep testing. U. S. Atomic Energy Commission Report IS-48. [Iowa State University of Science and Technology] 1959.

XI. ACKNOWLEDGMENTS

Sincere appreciation is extended to Dr. Robert Uhrig for his many suggestions and support throughout the investigation, to Dr. Glenn Murphy, Head of the Department of Theoretical and Applied Mechanics, who originally suggested the problem and maintained a continued interest, and to Jack R. Bohn for his assistance in developing the testing facility.